



HAL
open science

Stabilization of second-order non-minimum phase system with delay via PI controllers. Spectral abscissa optimization

Diego Torres-García, César-Fernando Méndez-Barrios, Silviu-Iulian Niculescu

► **To cite this version:**

Diego Torres-García, César-Fernando Méndez-Barrios, Silviu-Iulian Niculescu. Stabilization of second-order non-minimum phase system with delay via PI controllers. Spectral abscissa optimization. IEEE Access, 2024, pp.1-1. 10.1109/ACCESS.2024.3499748 . hal-04789103

HAL Id: hal-04789103

<https://hal.science/hal-04789103v1>

Submitted on 18 Nov 2024

HAL is a multi-disciplinary open access archive for the deposit and dissemination of scientific research documents, whether they are published or not. The documents may come from teaching and research institutions in France or abroad, or from public or private research centers.

L'archive ouverte pluridisciplinaire **HAL**, est destinée au dépôt et à la diffusion de documents scientifiques de niveau recherche, publiés ou non, émanant des établissements d'enseignement et de recherche français ou étrangers, des laboratoires publics ou privés.



Distributed under a Creative Commons Attribution - NonCommercial 4.0 International License

Date of publication xxxx 00, 0000, date of current version xxxx 00, 0000.

Digital Object Identifier 10.1109/ACCESS.2024.0429000

Stabilization of second-order non-minimum phase system with delay via PI controllers. Spectral abscissa optimization

DIEGO TORRES-GARCÍA^{1, 2}, CÉSAR-FERNANDO MÉNDEZ-BARRIOS¹, and SILVIU-IULIAN NICULESCU², (Fellow, IEEE)

¹Universidad Autónoma de San Luis Potosí (UASLP), Facultad de Ingeniería, Dr. Manuel Nava No.8, San Luis Potosí, S.L.P., México (e-mail: diego.torres@uaslp.mx, fernando.barrios@uaslp.mx)

²Université Paris-Saclay, CNRS, CentraleSupélec, Inria, Laboratoire des Signaux et Systèmes (L2S, UMR CNRS 8506), F-91192, Gif-sur-Yvette, France (e-mail: diego.torres-garcia@centralesupelec.fr, silviu.niculescu@centralesupelec.fr)

Corresponding author: Cesar-Fernando Méndez-Barrios (e-mail: fernando.barrios@uaslp.mx).

The work of Torres-García is supported by the "ADI 2022" project funded by the IDEX Paris-Saclay (France), ANR-11-IDEX-0003-02 and by CONACyT-UASLP (Mexico), CVU: 929482. The work of C.-F. Méndez-Barrios has been supported by CONAHcyT-México, under the grant *Ciencia Básica y de Frontera*: CBF2023–2024–2696.

ABSTRACT This paper addresses the stabilization of a general class of linear single-input/single-output (SISO) second-order non-minimum phase systems with input channel delays using Proportional-Integral (PI) controllers. Such systems arise in various applications, including power electronic circuits and biochemical reactors. The primary goal is to enhance system performance by determining optimal control gains that shift the spectral abscissa of the closed-loop system as far to the left as possible, thereby improving its decay rate. To achieve this, we introduce a geometric framework that characterizes the stability region of the closed-loop system in three distinct cases. Our main contribution is a systematic tuning approach to achieve the desired decay rate when feasible. Additionally, we discuss the controller's fragility and the delay margin of the closed-loop system to ensure practical applicability. The effectiveness of the proposed method is demonstrated through numerical simulations for each scenario. Finally, two practical case studies—a boiler steam drum and a DC-DC boost converter—are presented to illustrate the results' relevance in practice.

INDEX TERMS Linear systems, Non-minimum phase, PI control, Quasi-polynomials, Spectral abscissa, Time-delay

I. INTRODUCTION

IT is well known that second-order systems can model a wide variety of industrial processes [1]. One of the most common characteristics of such systems is the presence of unstable zeros, commonly referred to as non-minimum phase (NMP). When subjected to a classical step input, these NMP systems are characterized by an *undershoot* in the initial response, making them more challenging to control than those of minimum phase behavior. Additionally, dynamical systems often operate with input/output delays, which can arise from various sources such as material transport, delayed sensing, communication lags, and control decisions, among others [2]–[5]. Typical examples of second-order NMP systems with time delays include biochemical reactors, hydraulic turbines, airplanes, and power electronics converters, to name a few [6]–[10]. Therefore, given the large array of real-world processes that second-order NMP time-delay systems can

model, the problem of stabilizing them and improving their performance is of theoretical and practical interests.

Both phenomena mentioned above require special treatment when studying the closed-loop stability of the system. On the one hand, the presence of time delays makes the system infinite-dimensional, and the stability analysis becomes more challenging. More precisely, in the linear case, the characteristic function has an infinite number of characteristic roots, and the location of the roots depends on the system's parameters (including the delay). The problem of stabilizing a linear system in the presence of constant delays has been of interest in the last 70 years [11]–[15], and the use of the classical Proportional-Integral-Derivative controllers (PID) has proven to be effective in most cases [16]–[20]. On the other hand, the presence of unstable zeroes also increases the difficulty of controlling the system; in particular, in some cases, its control often requires the inclusion of the derivative

action.

This last requirement is especially challenging in the presence of time delays. Indeed, due to the system's structure under consideration, the inclusion of the derivative action will produce a closed-loop system of *neutral type*¹. This situation requires additional considerations and restricts the derivative gain by $|k_d| < 1$. Furthermore, recent research has focused on the *improperly-posedness* of the implementation of the derivative operator [21], [22], that is, even if the closed-loop system with the PID controller is stable, stability might be lost after replacing the derivative operator by the corresponding delay-difference approximation. This problem, as well as the well-known high-frequency noise amplification, can sometimes be tackled with the inclusion of low-pass filters. However, when the relative degree of the system equals one, as in the case of a second-order NMP system, it should be mentioned that the presence of the filter may destabilize the system (for further details, we refer to [23]). Moreover, in many real-world systems, measuring the derivative of the state might be unfeasible, and the corresponding controller cannot be explicitly implemented. Alternative approaches exist, but they lead to increasing complexity of the control scheme by increasing the number of parameters to be tuned, making the analysis more involved. In order to avoid such problems, we decided to drop the derivative action and, instead, look to optimize the performance of the system under the utilization of a classical PI controller.

It should be mentioned that considering a PI controller implies that only some of the systems with the proposed structure can be stabilized. It is essential to mention that this problem has been previously discussed in the literature. In fact, since the delay appears in the input-output channels, the simplest method was to exploit the structure of the interconnection by approximating the delay by a Padé approximation (see, for instance, [24]), that is:

$$e^{-\tau s} \approx \frac{\sum_{k=0}^N (-\tau s/2)^k / k!}{\sum_{k=0}^N (\tau s/2)^k / k!},$$

where N corresponds to the order of the approximation (for further details on this kind of analysis, see [4] and [5]). While such an approximation makes the system finite-dimensional, thereby simplifying the system's stability analysis, it may strongly affect the location of the characteristic roots of the original dynamical systems with respect to parameters' changes. Thus, it can result in mistuning the control parameters and making it difficult to estimate the closed-loop system decay rate.

It is worth noting that recent research efforts have also focused on the case of time-varying delays (see, for example, [25]). However, under such configurations, *imposing* a desired decay rate become more challenging. Fortunately, in some scenarios, one can consider an *averaging* approach to this problem (see, for instance, [26]). Moreover, as described in [27], one can *impose* a constant delay by inducing an

additional delay whenever the given delay is inferior to a certain upper bound $\bar{\tau}$, with the existence of such a bound as the only restriction. Given these observations, we opted to consider only static delays in our analysis.

The contribution of this paper is threefold:

First, the geometrical properties of the stability region in the control parameter space (k_p, k_i) are studied. In particular, the space is *partitioned* in several domains, each of them characterized by a fixed number of unstable roots. Therefore, the region of interest corresponds to the one characterized by zero unstable roots. Such a methodology, known as the \mathcal{D} -partition method, goes back to the pioneering work of Neimark (see, for instance, [28]). Similar ideas were also proposed by [29] with a detailed discussion of scalar and second-order delay systems in the corresponding parameter-space, but without any attempt to optimize the decay rate. It is worth mentioning that studying the stability properties of a system based on its parameters is an approach that has been deeply explored. Indeed, works such as [30] and [31] look to robustify the control scheme by studying the control parameter space. Others, such as [32], study the stability properties of time-delay systems with respect to the delay parameter, and the corresponding method is known as the τ -decomposition method. We refer to [33] for further details on such a methodology and, in particular, the idea to use the delay as a *control parameter*.

Second, we propose a methodology that allows finding, whenever it exists, the point inside the stable region that places the right-most root of the closed-loop system as far left as possible, improving its decay rate. A similar approach can be found in [34], where the system under consideration is also a second-order LTI system, but without addressing NMP behavior nor input/output delays). One interesting property is that one can optimize the spectral abscissa, thus the performance, of the closed-loop system using a low-order and low-complexity control law, such as a PI controller, even when the system is infinite-dimensional.

Third, the robustness of the closed-loop system with respect to (i) uncertainty of the control gains and (ii) the delay parameter are analyzed for the sake of applicability, with the remark that, as mentioned above into a different frame, one case further use the delay as a control parameter.

Finally, it should be mentioned that a first version of some of the results can be found in [35]. However, in contrast to the mentioned paper, a deeper discussion concerning the geometrical properties of the system's stability region is proposed. In particular, it is shown that whenever such a region exists, it is also unique. To the best of the authors' knowledge, such a finding represents a novelty in the open literature. Furthermore, a discussion around the maximum possible multiplicity of the system's characteristic roots under the considered configuration is also presented. Moreover, new results are discussed: first, the *fragility* problem of the PI controller is studied, that is, how robust the controller is with respect to control parameters uncertainties. Next, but in a similar spirit, the margin delay of the closed-loop system is also explicitly

¹that is, a system with a delay in the highest order derivative

computed. Finally, new numerical and practical examples were included to illustrate the presented results, as well as the corresponding proofs of the given results.

The structure of this paper is as follows: Section II defines the problem to be solved and outlines the necessary prerequisites. In Section III, we characterize the stability region of the closed-loop system within the control parameter space. Section IV presents the main results on the optimization of the spectral abscissa of the closed-loop system. Section V examines the robustness of the closed-loop system against uncertainties in the control gains, while Section VI addresses the delay margin of the system. To illustrate the presented results, Section VII includes several numerical examples. Finally, Section VIII provides two practical examples to demonstrate the effectiveness of the proposed results in real-world applications.

A. NOTATIONS

Throughout this paper, the following standard notations are used: the set of real numbers is denoted by \mathbb{R} . In particular, $\mathbb{R}_+ := \{x \in \mathbb{R} : x > 0\}$, and for any given set \mathcal{A} , $\mathcal{A}^* := \mathcal{A} \setminus \{0\}$. Next, $\mathbb{C} (\mathbb{C}_+, \mathbb{C}_-)$ represents the set of complex numbers (with strictly positive/negative real parts) and $i := \sqrt{-1}$. For a complex number $z \in \mathbb{C}$, \bar{z} represents its complex conjugate. For a real number x , $\text{sign}(x)$ denotes its sign, with $\text{sign}(x) \in \{0, \pm 1\}$. For two vectors \vec{x} and \vec{y} of the same dimensions, $\langle \vec{x}, \vec{y} \rangle$ represents the scalar product between them. Finally, for a given set \mathcal{A} , its cardinality is denoted by $\text{card}\{\mathcal{A}\}$.

II. PROBLEM FORMULATION AND PREREQUISITES

Consider a continuous Linear Time-Invariant (LTI) Single-Input/Single-Output (SISO) dynamical system of the form:

$$\Sigma : \begin{cases} \dot{x}(t) = Ax(t) + Bu(t - h), \\ y(t) = Cx(t), \end{cases} \quad (1)$$

including a delay in the input channel. The transfer function of the system writes as:

$$H_{yu}(s; h) := \frac{P(s)}{Q(s)} e^{-hs} \equiv C(sI - A)^{-1} B e^{-hs}, \quad (2)$$

where $h \in \mathbb{R}_+^*$ denotes the input delay, $P(s)$ and $Q(s)$ are polynomial functions in the complex variable s given by:

$$P(s) = s - z, \quad (3)$$

and

$$Q(s) = s^2 + as + b, \quad (4)$$

where $s = z$ is an unstable zero with $z > 0$ making the system NMP, $(a, b) \in \mathbb{R}^2$, and $Q(z) \neq 0$. This last condition rewrites as $z^2 + az + b \neq 0$ and simply states that the system realization is minimal in the sense that there is no pole-zero cancellation.

Consider now the system (2) in closed-loop with a standard PI controller $K(s)$. Its representation in frequency-domain writes as:

$$K(s) = k_p + \frac{k_i}{s}, \quad (5)$$

where $(k_p, k_i) \in \mathbb{R}^2$ are the controller's gains. With no lack of generality, we assume that $k_p k_i \neq 0$, but the proposed approach also covers the limit cases when $k_p = 0$ or $k_i = 0$. In particular, $k_i = 0$ corresponds to a proportional gain. In this last case, a detailed discussion of the stability regions of LTI SISO systems in the parameter space defined by the gain k_p and the delay h can be found in [33].

With the notations and remarks above, the characteristic function of the closed-loop system $\Delta : \mathbb{C} \times \mathbb{R}^2 \times \mathbb{R}_+ \rightarrow \mathbb{C}$ can be written as a function of the controller gains (k_p, k_i) and the delay h as follows:

$$\Delta(s; k_p, k_i, h) := s^3 + as^2 + bs + e^{-hs} (s - z) (k_p s + k_i), \quad (6)$$

which is a quasi-polynomial due to the presence of the exponential term. In other words, as discussed in the Introduction, we can further interpret the delay h as a system parameter.

It is well-known that Δ has an infinite number of characteristic roots, and, as in the finite-dimensional case, the stability properties follow from the location of such roots with respect to the imaginary axis of the complex plane. More precisely, the closed-loop system is stable iff all the characteristic roots have negative real parts. Furthermore, such roots depend continuously on the systems' parameters. For a deeper discussion of such quasi-polynomials, we refer to [11], [33] and the references therein.

The quasi-polynomial Δ has the following property:

Property 1: Let $\Psi \subset \mathbb{R}^2$ denote the set of all pairs (k_p, k_i) such that $k_i < 0$ and $k_p \geq 0$, and consider the quasi-polynomial $\Delta(s; k_p, k_i, h)$ given by (6). Then, for any given tuple $(a, b, z, h) \in \mathbb{R}^2 \times \mathbb{R}_+^2 \setminus \{(0, 0)\}$ and $(k_p, k_i) \notin \Psi$, there exist at least one $r \in \mathbb{R}$ such that the following holds:

$$\Delta(r; k_p, k_i, h) = 0. \quad (7)$$

Proof. We start by noting that for $s = 0$, the following holds:

$$\text{sign}(\Delta(0; k_p, k_i, h)) = -\text{sign}(k_i). \quad (8)$$

Additionally, for some sufficiently large $s = r^* \gg 0$, it is clear that $\Delta(r^*; k_p, k_i, h) > 0$. Therefore, if $k_i \geq 0$, by the Intermediate Value Theorem, it is clear that there exists at least one $r \in [0, r^*]$ that is a root of Δ . Next, if $k_i < 0$ and $k_p < 0$, then $\Delta(s; k_p, k_i, h) \rightarrow -\infty$ as $s \rightarrow -\infty$, and by the same arguments, we know that there must exist some $r \in (-\infty, 0)$ that is a root of Δ . QED.

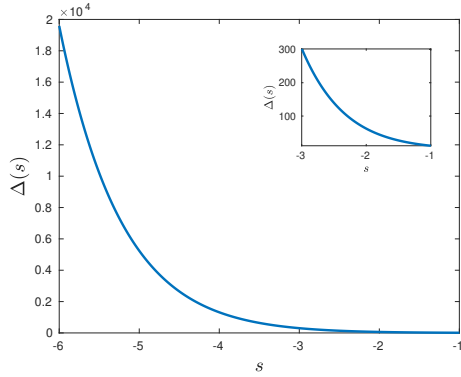
Remark 1: Let $\Delta(s; k_p, k_i, h)$ given by (6). Then, $k_i < 0$ is a necessary condition for the stability of the closed-loop system.

Remark 2: Although the delay-free closed-loop system always has at least one real root, it is possible to have configurations such that in the time-delay case, for a given delay value, the closed-loop system does not present any real characteristic root. Consider, for example, the following closed-loop characteristic function (with $h = 1$):

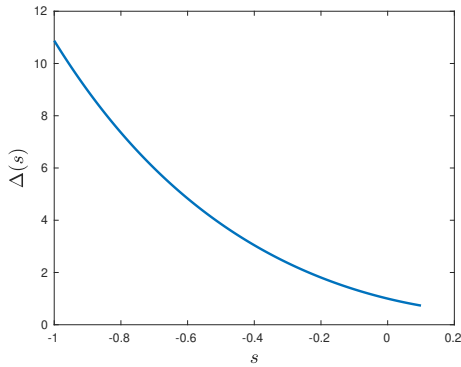
$$\Delta(s) = f_1(s) + e^{-s} f_2(s) = s(s+1)(s-0.1) + e^{-s}(s-1)^2 \quad (9)$$

It is clear that $e^{-s} f_2(s)$ is positive for any $s \in \mathbb{R}$, except for $s = 1$, for which it is also easy to observe that $\Delta(1) > 0$. Next,

$f_1(s)$ is negative for $s \in (0, 0.1)$ and for any $s \in (-\infty, -1)$, therefore, any solution of $\Delta(s) = 0$ has to be in those intervals. One can also note that, as $s \rightarrow -\infty$, $e^{-s}f_2(s) \rightarrow \infty$, and that for $s = -1$ we have $ef_2(-1) = 4e$. The plot of $\Delta(s)$ for $s \in (-1, 0.1)$ and $(-6, -1)$ is depicted in Figure 1. This particular behavior can be explained by observing the



(a) Behavior of $\Delta(s)$ for $s < -1$.



(b) Behavior of $\Delta(s)$ for $s \in (-1, 0.1)$.

FIGURE 1. Behavior of quasi-polynomial (9) for s real.

evolution of the system roots as we increase the parameter h from 0 to $1/3$, as shown in Figure 2. More precisely, when the delay h is increased from 0 to $1/3$, there is a splitting of a double real (negative) characteristic root in a pair of complex conjugate roots.

Next, before stating the problem formulation, we introduce the notions of spectral abscissa (that is, the rightmost characteristic root) and σ -stability:

Definition 1 (Spectral abscissa [33]): For the closed-loop system (2)-(5) with associated characteristic function Δ given by (6), its spectral abscissa is defined by the real number:

$$\rho(\Delta) = \max \{ \Re(s_0) : s_0 \in \mathbb{C}, \Delta(s_0; k_p, k_i, h) = 0 \}$$

Remark 3: As discussed in [33], in the retarded case, the spectral abscissa function is continuous, bounded, and finite. For a given set of parameters (k_p, k_i, h) , the stability of the closed-loop function holds iff the spectral abscissa satisfies the inequality $\rho(\Delta) < 0$.

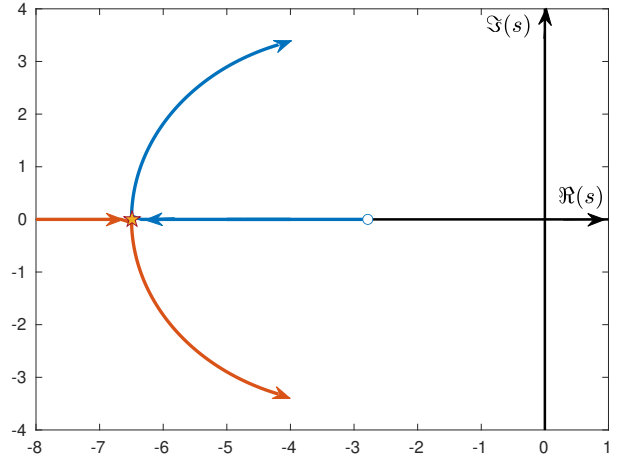


FIGURE 2. Roots of quasi-polynomial (9) as h increases in $(0, 1/3)$.

Definition 2 (σ -stability [33]): Let $\sigma \in \mathbb{R}_+$ be a strictly positive real number. Then the closed-loop system (2)-(5) is said to be σ -stable if its spectral abscissa $\rho(\Delta)$ verifies the inequality $\rho(\Delta) \leq -\sigma$.

Remark 4: It is easy to observe that, in the limit case, $\sigma = 0$, the closed-loop may have characteristic roots on the imaginary axis corresponding to a marginally stable system if the characteristic roots are simple.

It is worth bearing the following definition in mind:

Definition 3 (Quasi-polynomial degree [36]): Consider a quasi-polynomial $\Delta : \mathbb{C} \rightarrow \mathbb{C}$ of the following form:

$$\Delta(s) := \sum_{j=0}^m P_j(s)e^{-h_j s},$$

where P_j for $j \in \{0, 1, \dots, m\}$ are polynomials in s with real coefficients, and $h_j \in \mathbb{R}_+$ such that $h_0 = 0 < h_1 < h_2 < \dots < h_m$. The degree of Δ is given by:

$$\deg(\Delta) = m + \sum_{j=0}^m d_j,$$

where $d_j = \deg(P_j)$, for all $j = 0, 1, \dots, m$.

In our case, it is easy to observe that $\deg(\Delta) = 3 + 2 + 1 = 6$. From previous works, such as [34], [37], and Remark 8 from [38], one could imagine that the optimal spectral abscissa always corresponds to a root with maximum multiplicity. However, this is not always the case. It is also known from [39] that for a given quasi-polynomial Δ with $\deg(\Delta) = d$, a root with maximum multiplicity always corresponds to a dominant one, but whether or not this implies that such a spectral abscissa is optimal needs a better understanding of the underlying mechanism.

A. PROBLEM FORMULATION

Bearing in mind the above definitions, observations, and remarks, the problem we aim to address is the following:

Problem 1: For a second-order NMP LTI SISO system with transfer function given by (2) in closed-loop with a PI controller given by (5), find the gains $(\hat{k}_p, \hat{k}_i) \in \mathbb{R}^2$ such that the spectral abscissa of the closed-loop system achieves its minimal value.

B. MOTIVATING EXAMPLE

To illustrate the main idea of the problem that is addressed in this paper, consider the NMP second-order system described by the following transfer function:

$$H_{yu}(s; h) = \frac{s - 2}{(s + 1)^2} e^{-s}, \tag{10}$$

which corresponds to an open-loop stable system. Taking the PI controller $K(s) = k_p + k_i/s$, it is easy to see that, despite the presence of the unstable zero, there exist certain pairs $(k_p, k_i) \in \mathbb{R}^2$ such that the stability is preserved in closed-loop. Nonetheless, not all the stabilizing controllers will produce the same response. Indeed, consider the two following pairs $(k_{p1}, k_{i1}) = (-0.1031, -0.0819)$ and $(k_{p2}, k_{i2}) = (-1/2, -1/6)$, both preserving closed-loop stability. Figure (3) depicts the error signal $e(t) = r(t) - y(t)$ with $r(t) = 1$ for all $t > 0$ and $r(t) = 0$ otherwise.

Note that the closed-loop system under consideration is a linear time-delay system of the *retarded* type; therefore, if all its characteristic roots have negative real parts, the system is *exponentially* stable. It is easy to conclude that the exponential decay rate, that is, the *velocity* with which the error signal goes to zero, is a function of the particular choices of the controller gains. More precisely, such a decay rate depends on the location of the closed-loop system spectral abscissa, which in this case corresponds to $\rho(\Delta) = -0.5043$ for (k_{p1}, k_{i1}) and $\rho(\Delta) = -0.1270$ for (k_{p2}, k_{i2}) .

In the following, we aim to find a systematic procedure that allows finding the optimal values of the controller gains, such that spectral abscissa is as far left as possible, that is, *optimizing the spectral abscissa as a function of the controller gains*.

III. GEOMETRY OF THE STABILITY REGION

Bearing to mind the continuity property of the characteristic roots of the closed-loop system (2)-(5) with respect to the system's parameters ², we note that a characteristic root can only cross from the left-half plane to the right-half plane (stability to instability), or from the right-half plane to the left-half plane (instability to stability), by crossing the imaginary axis. We introduce the notions of frequency sweeping set and curves in a similar way as in [40]:

Definition 4 (Frequency crossing set): The frequency crossing set $\Omega \subset \mathbb{R}$ is the set of all ω such that, for a given h , there exist at least one pair of control gains $(k_p, k_i) \in \mathbb{R}^2$ such that

$$\Delta(i\omega; k_p, k_i, h) = 0. \tag{11}$$

²More precisely, these roots are continuous functions of the system parameters [33]

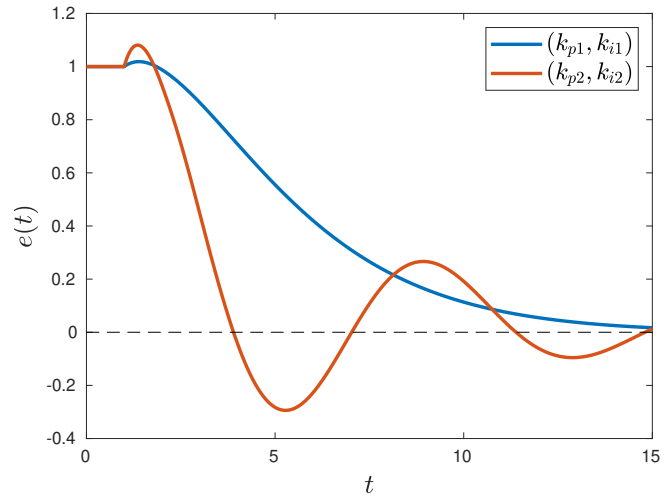


FIGURE 3. Error signal produced by two different controllers (k_p, k_i) .

Remark 5: Note that $\Delta(i\omega; k_p, k_i, h) = 0$ implies that $\Delta(-i\omega; k_p, k_i, h) = 0$, therefore in the remaining part of the paper we will consider only positive frequencies.

Definition 5 (Stability crossing curves): The stability crossing curve \mathcal{K} is the set of all pairs $[k_p, k_i]^T \in \mathbb{R}^2$ for which there exist $\omega \in \Omega$. Any point $\vec{k} \in \mathcal{K}$ is referred to as a crossing point.

Proposition 1 (Crossing points characterization): Consider the system described by the transfer function (2) in closed-loop with the PI controller (5). Then, the crossing points $\vec{k} = (k_p(\omega), k_i(\omega)) \in \mathbb{R}^2$ are given by:

$$k_p(\omega) = \frac{\omega \sin(h\omega)\alpha_1 + \cos(h\omega)\alpha_2}{\omega^2 + z^2}, \tag{12}$$

$$k_i(\omega) = \frac{\omega (\sin(h\omega)\alpha_3 + \omega \cos(h\omega)\alpha_4)}{\omega^2 + z^2}, \tag{13}$$

where $\alpha_1 = (\omega^2 - az - b)$, $\alpha_2 = (bz - \omega^2(a + z))$, $\alpha_3 = (\omega^2(a + z) - bz)$ and $\alpha_4 = (\omega^2 - az - b)$. Furthermore, if $\omega = 0$, we have $k_i = 0$.

Proof. The proof follows straightforwardly by noting that if $\Delta(i\omega; k_p, k_i, h) = 0$ then:

$$\Re \{ \Delta(i\omega; k_p, k_i, h) \} = \Im \{ \Delta(i\omega; k_p, k_i, h) \} = 0.$$

QED.

Corollary 0.1: Consider the system described by the transfer function $H_{yu}(s; h)$ given by (2) in closed-loop with the PI controller in (5), then the stability crossing curve $\mathcal{K} = \mathcal{K}_\omega \cup \mathcal{K}_0$ is given by:

$$\mathcal{K}_\omega := \{ \vec{k} \in \mathbb{R}^2 : \vec{k} := (k_p(\omega), k_i(\omega)), \forall \omega \in \Omega \},$$

$$\mathcal{K}_0 := \{ \vec{k} \in \mathbb{R}^2 : \vec{k} := (k_p, 0), k_p \in \mathbb{R} \}.$$

It is worth mentioning that the crossing curve \mathcal{K} decomposes the parameter space into disjoint regions characterized by the same number of unstable roots. We refer to the region, if any,

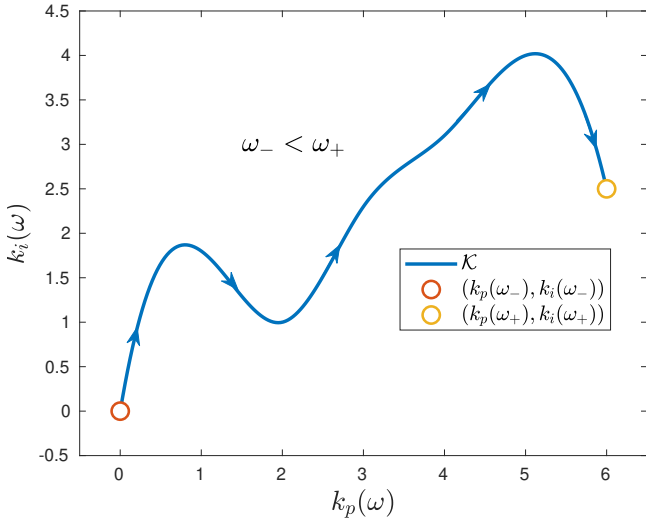


FIGURE 4. Positive direction of the curve \mathcal{K} .

for which there are no unstable roots as the *stable region*, denoted by \mathcal{S} .

A. CROSSING DIRECTIONS

In the following, we refer to the direction of the curve \mathcal{K} that corresponds to increasing ω as the *positive direction* of the curve, and we illustrate this idea in Figure 4. We have the following result:

Proposition 2: Consider the system described by the transfer function $H_{yu}(s; h)$ in (2) in closed-loop with the PI controller (5). Then, a pair of characteristic roots cross the imaginary axis from \mathbb{C}_+ to \mathbb{C}_- (\mathbb{C}_- to \mathbb{C}_+) if \vec{k} traverses the stability crossing curve \mathcal{K} from left to right (right to left) with respect to the positive direction of the curve.

Proof. The proof is given constructively. Consider the characteristic function $\Delta(s; k_p, k_i, h)$. Next, consider the change of variable $s \rightarrow s - \sigma$, with $\sigma \in \mathbb{R}$. Note that, under this change of variable, we can produce two different crossing curves. First, the crossing curve \mathcal{K}_ω , corresponding to fixed $\sigma = \sigma^* \in \mathbb{R}_+$, and second, \mathcal{K}_σ , this time with respect to σ and for $\omega = \omega^* \in \mathbb{R}_+$ fixed. Now, the tangent to the crossing curve \mathcal{K}_ω is given by $\vec{t} = (dk_p/d\omega, dk_i/d\omega)^T$, while the tangent to the curve \mathcal{K}_σ is given by $\vec{t}_\sigma = (dk_p/d\sigma, dk_i/d\sigma)^T$. Since the curve \mathcal{K}_ω considers $\omega \in \mathbb{R}_+$, there exists a point where both curves cross each other. At that exact point, consider the inner product between the normal to the tangent \vec{t} , pointing to the left, with respect to the positive direction of the curve, that is $\vec{n}_t = (-dk_i/d\omega, dk_p/d\omega)$, and the tangent \vec{t}_σ , leading to:

$$\langle \vec{n}_t, \vec{t}_\sigma \rangle = \frac{dk_p}{d\omega} \frac{dk_i}{d\sigma} - \frac{dk_i}{d\omega} \frac{dk_p}{d\sigma}.$$

Next, if the crossing is always occurring in the same direction, $\text{sign}(\langle \vec{n}_t, \vec{t}_\sigma \rangle)$ must remain constant. Consider the total

derivative w.r.t. ω on $\Delta(i\omega - \sigma^*; k_p, k_i, h) = 0$, that is:

$$i \frac{\partial \Delta}{\partial \omega} + \frac{\partial \Delta}{\partial k_p} \frac{dk_p}{d\omega} + \frac{\partial \Delta}{\partial k_i} \frac{dk_i}{d\omega} = 0,$$

and consider the following definitions:

$$R_0 + iI_0 = i \frac{\partial \Delta}{\partial \omega}, \quad (14)$$

$$R_1 + iI_1 = - \frac{\partial \Delta}{\partial k_p}, \quad (15)$$

$$R_2 + iI_2 = - \frac{\partial \Delta}{\partial k_i}, \quad (16)$$

from which we obtain the following representation:

$$\begin{pmatrix} R_1 & R_2 \\ I_1 & I_2 \end{pmatrix} \begin{pmatrix} \frac{dk_p}{d\omega} \\ \frac{dk_i}{d\omega} \end{pmatrix} = \begin{pmatrix} R_0 \\ I_0 \end{pmatrix},$$

which allows us to write $\vec{t} = (dk_p/d\omega, dk_i/d\omega)^T$ in the following way:

$$\vec{t} = \frac{1}{R_1 I_2 - R_2 I_1} \begin{pmatrix} R_0 I_2 - R_2 I_0 \\ R_1 I_0 - I_1 R_0 \end{pmatrix},$$

provided that $R_1 I_2 - R_2 I_1 \neq 0$. Similarly, we consider the total derivative w.r.t. σ on $\Delta(i\omega^* - \sigma; k_p, k_i, h) = 0$, and by a similar procedure, one can arrive at the following definitions:

$$R_\sigma + iI_\sigma = i \frac{\partial \Delta}{\partial \sigma}, \quad (17)$$

$$R_1 + iI_1 = - \frac{\partial \Delta}{\partial k_p}, \quad (18)$$

$$R_2 + iI_2 = - \frac{\partial \Delta}{\partial k_i}. \quad (19)$$

Note that at the point where both curves cross $R_\sigma = -I_0$ and $I_\sigma = R_0$, therefore:

$$\vec{t}_\sigma = \frac{1}{R_1 I_2 - R_2 I_1} \begin{pmatrix} R_0 R_1 + I_0 I_1 \\ -R_0 R_2 - I_0 I_2 \end{pmatrix},$$

provided that $R_1 I_2 - R_2 I_1 \neq 0$. One then can compute $\langle \vec{n}_t, \vec{t}_\sigma \rangle$:

$$\langle \vec{n}_t, \vec{t}_\sigma \rangle = \frac{R_0^2 + I_0^2}{R_1 I_2 - R_2 I_1},$$

which implies that $\text{sign}(\langle \vec{n}_t, \vec{t}_\sigma \rangle) = \text{sign}(R_1 I_2 - R_2 I_1)$, which is easy to compute:

$$\begin{aligned} R_1 I_2 - R_2 I_1 &= -\omega (e^{2h\sigma}) (\omega^2 + (\sigma + z)^2) \\ &\implies \text{sign}(R_1 I_2 - R_2 I_1) = -1. \end{aligned}$$

The sign is not only constant but negative; this ends the proof. QED.

Remark 6: Note that Proposition 2 implies that the stable region \mathcal{S} , if any, will always be the *most inner* region.

Proposition 3: Consider the system described by the transfer function $H_{yu}(s; h)$ in (2) in closed-loop with the PI controller (5). Then, a real characteristic root crosses from \mathbb{C}_+ to \mathbb{C}_- (\mathbb{C}_- to \mathbb{C}_+) if \vec{k} traverses the stability crossing curve \mathcal{K}_0 from

up to down at any crossing point located to the right (left) of k_0 given by:

$$\vec{k}_0 = \begin{bmatrix} k_{p0} \\ k_{i0} \end{bmatrix} = \begin{bmatrix} b/z \\ 0 \end{bmatrix}.$$

Proof. First, note that \mathcal{K}_0 is given by the horizontal axis of the parameters plane (k_p, k_i) , i.e., it is defined by $k_i = 0$. Next, employing the implicit function theorem (see, for instance, [41]), we have:

$$\frac{ds}{dk_i} = \frac{z-s}{d_1 s e^{hs} + b e^{hs} + h k_i (z-s) - k_p d_2 + k_i},$$

where $d_1 = 2a + 3s$, $d_2 = (s(h(s-z) - 2) + z)$, and we have $\Delta(s=0, k_p, k_i=0, h) = 0$, thus:

$$\text{sign} \left(\frac{ds}{dk_i} \right) \Big|_{s=0, k_i=0} = \text{sign}(b - k_p z).$$

By definition, $z > 0$; therefore, the crossing changes its sign exactly at $k_p = b/z$. This last observation ends the proof. QED.

B. DIRECTION OF MOVEMENT

Now that the crossing curves have been characterized, we are interested in characterizing the direction in which the given curves *move* as the imaginary axis is shifted to the left on the complex plane. We have the following result:

Proposition 4: Consider the system described by the transfer function $H_{yu}(s; h)$ in (2) in closed-loop with the PI controller (5) with characteristic function $\Delta(s; k_p, k_i, h)$ given by (6). Then, if a region exists inside the control parameter space (k_p, k_i) such that all the characteristic roots are located inside \mathbb{C}_- , then such a region is unique.

Proof. Consider the change of variable $s \rightarrow s - \sigma$; when evaluating over the imaginary axis, the produced equation has the following form:

$$Q(i\omega - \sigma) + ((i\omega - \sigma) - z)(k_p(i\omega - \sigma) + k_i)e^{-h(i\omega - \sigma)} = 0.$$

This equation can be rewritten in the following way:

$$\begin{aligned} e^{h\sigma}(\cos(h\omega) - i \sin(h\omega))(k_p(i\omega - \sigma) + k_i) \\ = \frac{Q(i\omega - \sigma)(z + \sigma + i\omega)}{\sigma^2 + \omega^2 + z^2 + 2\sigma z}, \end{aligned}$$

which implies:

$$\begin{aligned} e^{h\sigma}(\cos(h\omega)(k_i - k_p\sigma) + k_p\omega \sin(h\omega)) \\ = \Re \left\{ \frac{Q(i\omega - \sigma)(z + \sigma + i\omega)}{\sigma^2 + \omega^2 + z^2 + 2\sigma z} \right\} =: \gamma, \end{aligned}$$

and

$$\begin{aligned} e^{h\sigma}(\sin(h\omega)(k_p\sigma - k_i) + k_p\omega \cos(h\omega)) \\ = \Im \left\{ \frac{Q(i\omega - \sigma)(z + \sigma + i\omega)}{\sigma^2 + \omega^2 + z^2 + 2\sigma z} \right\} =: \beta, \end{aligned}$$

leading to:

$$k_p(\omega, \sigma) = \frac{e^{-h\sigma}(\gamma \sin(h\omega) + \beta \cos(h\omega))}{\omega}, \quad (20)$$

and

$$k_i(\omega, \sigma) = \frac{e^{-h\sigma} \cos(h\omega)(\tan(h\omega)(\gamma\sigma - \beta\omega) + \gamma\omega + \beta\sigma)}{\omega}. \quad (21)$$

Finally, we can express the curve composed by the corresponding points $(k_p, k_i) \in \mathbb{R}^2$ as:

$$\mathcal{K}(\omega, \sigma) := \begin{bmatrix} k_p(\omega, \sigma) \\ k_i(\omega, \sigma) \end{bmatrix} \equiv \frac{e^{-h\sigma}}{\omega} \begin{bmatrix} k_{11} & k_{12} \\ k_{21} & k_{22} \end{bmatrix} \begin{bmatrix} \gamma \\ \beta \end{bmatrix},$$

where

$$\begin{aligned} k_{11} &= \sin(h\omega), & k_{21} &= \cos(h\omega)(\sigma \tan(h\omega) + \omega), \\ k_{12} &= \cos(h\omega), & k_{22} &= \cos(h\omega)(\sigma - \omega \tan(h\omega)). \end{aligned}$$

Now that we have this representation, we introduce the following functions $u : \mathbb{R}_+ \times \mathbb{R}^2 \times \mathbb{R}_+ \rightarrow \mathbb{R}$ and $v : \mathbb{R}_+ \times \mathbb{R}^2 \times \mathbb{R}_+ \rightarrow \mathbb{R}$:

$$u(\omega; k_p, k_i, \sigma) := e^{h\sigma}(\cos(h\omega)(k_i - k_p\sigma) + k_p\omega \sin(h\omega)) - \gamma,$$

$$v(\omega; k_p, k_i, \sigma) := e^{h\sigma}(\sin(h\omega)(k_p\sigma - k_i) + k_p\omega \cos(h\omega)) - \beta$$

such that: $\Delta(i\omega - \sigma; h) = u(\omega; k_p, k_i, \sigma) + iv(\omega; k_p, k_i, \sigma)$. The total derivatives of u and v write as follows:

$$\begin{aligned} e^{h\sigma}(\omega \sin(h\omega) - \sigma \cos(h\omega))dk_p \\ + e^{h\sigma} \cos(h\omega)dk_i + \frac{\partial u}{\partial \sigma}d\sigma + \frac{\partial u}{\partial \omega}d\omega = 0, \\ e^{h\sigma}(\sigma \sin(h\omega) + \omega \cos(h\omega))dk_p \\ - e^{h\sigma} \sin(h\omega)dk_i + \frac{\partial v}{\partial \sigma}d\sigma + \frac{\partial v}{\partial \omega}d\omega = 0. \end{aligned}$$

which leads to the following representation of (dk_p, dk_i) :

$$\begin{bmatrix} dk_p \\ dk_i \end{bmatrix} = -\frac{\cos(h\omega)}{e^{h\sigma}\omega} \begin{bmatrix} dk_{11} & dk_{12} \\ dk_{21} & dk_{22} \end{bmatrix} \begin{bmatrix} \frac{\partial u}{\partial \sigma} & \frac{\partial u}{\partial \omega} \\ \frac{\partial v}{\partial \sigma} & \frac{\partial v}{\partial \omega} \end{bmatrix} \begin{bmatrix} d\sigma \\ d\omega \end{bmatrix},$$

where

$$\begin{aligned} dk_{11} &= \tan(h\omega), & dk_{21} &= \omega + \sigma \tan(h\omega), \\ dk_{12} &= 1, & dk_{22} &= \sigma - \omega \tan(h\omega). \end{aligned}$$

From Cauchy-Reimann equations we have the following relations:

$$\frac{\partial u}{\partial \sigma} = \frac{\partial v}{\partial \omega} \quad \text{and} \quad \frac{\partial u}{\partial \omega} = -\frac{\partial v}{\partial \sigma}.$$

Therefore we can write $[dk_p, dk_i]^T$ in the following way:

$$\begin{bmatrix} dk_p \\ dk_i \end{bmatrix} = \frac{-1}{e^{h\sigma}\omega} \begin{bmatrix} a_{11} & a_{12} \\ a_{21} & a_{22} \end{bmatrix} \begin{bmatrix} \frac{\partial u}{\partial \sigma} & \frac{\partial u}{\partial \omega} \\ -\frac{\partial u}{\partial \omega} & \frac{\partial u}{\partial \sigma} \end{bmatrix} \begin{bmatrix} d\sigma \\ d\omega \end{bmatrix},$$

where:

$$\begin{aligned} a_{11} &= \sin(h\omega), & a_{21} &= \omega \cos(h\omega) + \sigma \sin(h\omega), \\ a_{12} &= \cos(h\omega), & a_{22} &= \sigma \cos(h\omega) - \omega \sin(h\omega). \end{aligned}$$

Computing the Jacobian determinant one obtains:

$$\begin{aligned} \det(J(\mathcal{K}(\omega, \sigma))) &= -\frac{e^{-h\sigma}}{\omega} (-\omega \sin^2(h\omega) - \omega \cos^2(h\omega)) \\ &\quad \times \left[\left(\frac{\partial u}{\partial \sigma} \right)^2 + \left(\frac{\partial u}{\partial \omega} \right)^2 \right] \\ &= e^{-h\sigma} \left[\left(\frac{\partial u}{\partial \sigma} \right)^2 + \left(\frac{\partial u}{\partial \omega} \right)^2 \right], \end{aligned}$$

which is always positive, indicating that the curve $\mathcal{K}(\omega, \sigma)$ always preserves orientation as (ω, σ) change. This last observation ends the proof. QED.

C. STABILITY INDEX COMPUTATION

In the following, we aim to compute the stability index of a given region in the space of parameters (k_p, k_i) , that is, for a given $\vec{k}^* = [k_p^*, k_i^*]^T \notin \mathcal{K}$ compute the number of unstable characteristic roots n , which we know to be invariant inside a region. For such a task, we also define n_0 as the number of unstable roots associated with the origin \mathcal{O} , that is, the number of unstable roots when $\vec{k} = [0, 0]^T$. Note that $n_0 \in \{0, 1, 2\}$ is given by the number of unstable roots of $Q(s)$. Next, consider the line segment $\mathcal{O}\vec{k}^*$ connecting \mathcal{O} and \vec{k}^* . Such a line intersects the stability crossing curve \mathcal{K}_ω whenever $\vec{k} = \varepsilon \vec{k}^*$ with $\varepsilon \in (0, 1)$, i.e. whenever the vector defining the corresponding crossing point and \vec{k}^* are parallel. Moreover, since the line containing the segment $\mathcal{O}\vec{k}^*$ is given by $k_i = (k_i^*/k_p^*)k_p$, the corresponding $\omega = \omega^* \in \Omega$ for which the intersection occurs must fulfill the following equation:

$$k_p^* k_i(\omega^*) - k_i^* k_p(\omega^*) = 0, \quad (22)$$

and we will refer to the set of all ω^* for which (22) holds as $\Omega^* \subseteq \Omega$. Additionally, we consider the following indicator function $\mathcal{I} : \mathbb{R} \times \mathbb{R}^2 \times \Omega^* \rightarrow \{0, \pm 1\}$:

$$\mathcal{I}(\varepsilon, k_p^*, k_i^*, \omega^*) := \begin{cases} \text{sign}(\delta), & \text{if } \varepsilon \in (0, 1) \\ 0, & \text{if } \varepsilon \notin (0, 1), \end{cases} \quad (23)$$

where:

$$\delta = \left. \frac{ds}{dk_i} \right|_{s=i\omega^*, k_p=\varepsilon k_p^*, k_i=\varepsilon k_i^*},$$

where ds/dk_i can be obtained via the implicit function theorem. Next, we have three possible cases:

- 1) The crossing curve \mathcal{K}_ω starts at the origin \mathcal{O} if $b = 0$ since at $\omega = 0$ the crossing points are given by:

$$k_i(0) = 0 \quad \wedge \quad k_p(0) = \frac{b}{z}.$$

Therefore, in this case $n_0 = 1$ if $a < 0$ and $n_0 = 0$ otherwise.

- 2) The crossing curve \mathcal{K}_ω passes through the origin \mathcal{O} at $\omega \neq 0$ if $a = 0$ and $b > 0$, since the crossing points read:

$$k_p(\omega) = \frac{(b - \omega^2)(z \cos(h\omega) - \omega \sin(h\omega))}{\omega^2 + z^2},$$

and

$$k_i(\omega) = \frac{\omega(\omega^2 - b)(\omega \cos(h\omega) + z \sin(h\omega))}{\omega^2 + z^2},$$

therefore $k_p(\omega) = k_i(\omega) = 0$ at $\omega = \sqrt{b}$.

- 3) The crossing curve \mathcal{K}_ω never touches the origin \mathcal{O} , and n equals the number of unstable roots of $Q(s)$.

With this in mind, we have the following result.

Proposition 5: Let $\vec{k}^* := [k_p^*, k_i^*] \notin \mathcal{K}$ be an arbitrary pair in the parameter plane (k_p, k_i) . Then, for any given \vec{k}^* , the number of unstable characteristic roots n is given by:

$$n = n_0 + 2 \sum_{\omega \in \Omega^*} \mathcal{I}(\varepsilon, k_p^*, k_i^*, \omega). \quad (24)$$

Proof. Consider the characteristic quasi-polynomial $\Delta(s; k_p, k_i, h)$. It is clear that for $k_p = 0$ and $k_i = 0$, the characteristic roots will correspond to those of $Q(s)$, and by continuity arguments, the number of unstable roots of the closed-loop characteristic quasi-polynomial will remain constant unless a crossing of the stability crossing curve \mathcal{K} occurs. Next, since \mathcal{K} corresponds to the horizontal axis of the parameter plane (k_p, k_i) , it is clear that, as we move over the line segment $\mathcal{O}\vec{k}^*$ every crossing, if any, will be through \mathcal{K}_ω , which by the \mathcal{D} -partition theory correspond to a complex conjugate root crossing. Finally, it is clear that \mathcal{I} characterizes the direction of the crossing depending on the sign of the derivative. QED.

IV. OPTIMIZATION OF THE SPECTRAL ABCISSA

Before presenting the main result, we introduce the following notion:

Definition 6 (Self-intersection): We say that the stability crossing curve \mathcal{K} has a self-intersection if there exist a pair $(\omega_-, \omega_+) \in \mathbb{R}_+^2$ such that $\omega_- < \omega_+$ and:

$$k_p(\omega_-) \equiv k_p(\omega_+) \quad \wedge \quad k_i(\omega_-) \equiv k_i(\omega_+), \quad (25)$$

where $k_p(\cdot)$ and $k_i(\cdot)$ are crossing points given by (12) and (13), respectively.

Next, from the Routh-Hurwitz criterion, we note that in the delay-free case, the following inequalities must hold to stabilize the system:

$$0 < z(az + b), \quad (26)$$

$$-a < k_p < \frac{b}{z}, \quad (27)$$

$$\frac{(a + k_p)(k_p z - b)}{a + k_p + z} < k_i < 0. \quad (28)$$

In the rest of this paper, we have the following assumptions:

- A1 There exists a pair $(k_p, k_i) \in \mathbb{R}^2$ such that inequalities (26)-(28) hold.

Remark 7: Note that even in the delay-free case, the stability region is bounded, similar to what we expect in the time-delay case. In Figure 5, an example of the difference in the stability boundaries between the delay-free system and the time-delay

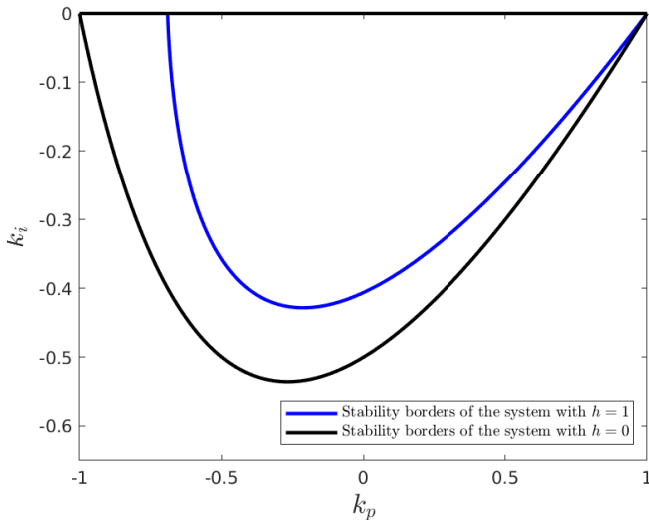
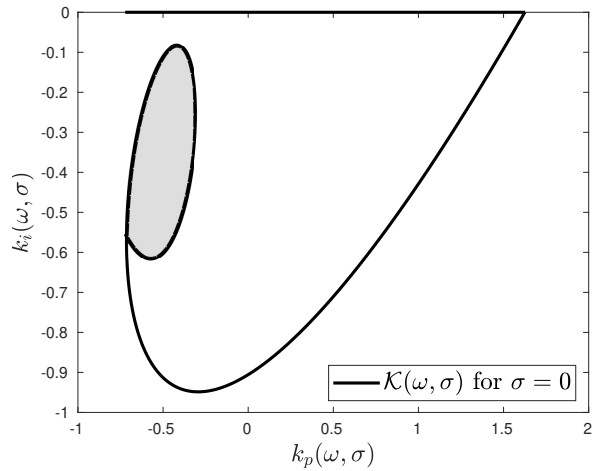
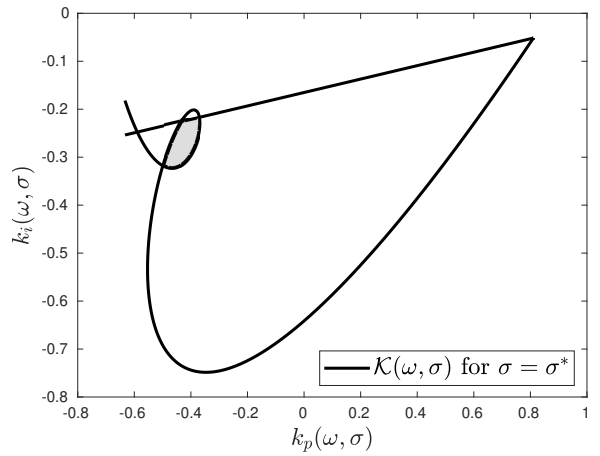


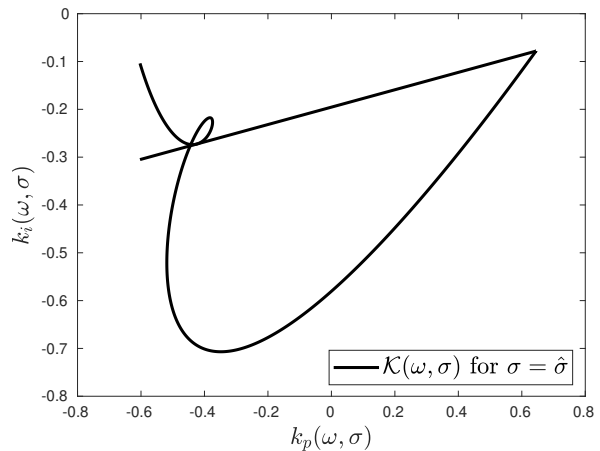
FIGURE 5. Comparison of the stability borders of the system when we consider the delay and when we assume it to be free of input delay.



(a) Stability region of the closed-loop system.



(b) σ -stable region for $\sigma^* < \hat{\sigma}$.



(c) Point of collapse.

FIGURE 7. Change in the stability region as σ increases.

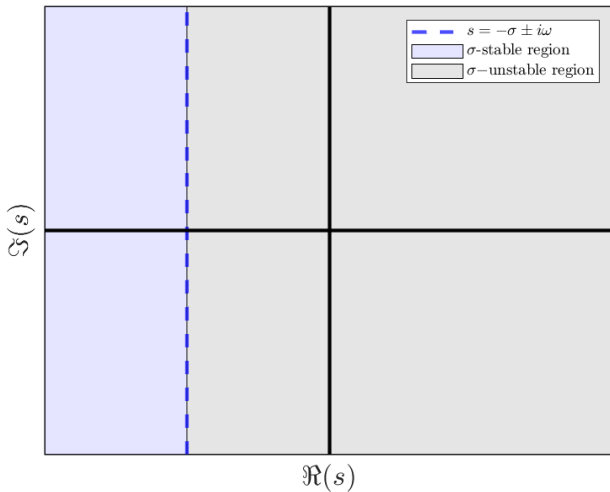


FIGURE 6. Stability with respect to the σ -axis.

one is depicted. As expected intuitively in our case, we can observe that the stability region of the time-delay system lies inside the delay-free one, emphasizing the importance of considering the delay term in the stability analysis.

A. COLLAPSE OF THE STABILITY REGION

In the following, we aim to detect the exact point inside the stability region at which the spectral abscissa reaches its minimal value. Note that by considering the change of variable $s \rightarrow s - \sigma$, one can study the σ -stability of the closed-loop system. In other words, we study the system's stability with respect to the σ -axis (see Figure 6). The main idea of this section is to propose a methodology that allows the identification of the maximum possible value of σ such that there exists at least one pair of control parameters (k_p, k_i) that σ stabilize a system with the form of (2).

In this spirit, we have the following result.

Theorem 1 (Optimal σ in the self-intersection free case): Consider the system described by the transfer function $H_{yu}(s; h)$

in (2) in closed-loop with the PI controller (5), and assume that the corresponding crossing curve \mathcal{K} does not have self-intersections, then the spectral abscissa $\rho(\Delta)$ achieves its minimum value $\hat{\sigma}$ at the smallest real positive root of the following fifth-order polynomial:

$$p(\sigma) := \sigma^5 + a_4\sigma^4 + a_3\sigma^3 + a_2\sigma^2 + a_1\sigma + a_0, \quad (29)$$

where:

$$\begin{aligned} a_4 &= 2z - a - \frac{4}{h}, & a_3 &= z(z - 2a) + b + \frac{2}{h^2} - \frac{2(a - 5z)}{h}, \\ a_2 &= \frac{z(-hz(ah + 6) + 6ah + 2bh^2 + 6)}{h^2}, \\ a_1 &= \frac{z(2z(2ah + 3) + bh(hz - 2))}{h^2}, & a_0 &= -\frac{2z(az + bhz + b)}{h^2}. \end{aligned}$$

Moreover, the point corresponds to a triple real root. *Remark 8:* Note that in the case where both roots of $Q(s)$ are negative (open-loop stable system), we have $a > 0$ and $b > 0$. Therefore, $a_0 < 0$, and since $p(\sigma)$ in (29) is monic, there would be at least two coefficients with different signs, and from the Descartes' rule (see [42]), we will have at least one real positive root.

Proof. From a geometrical observation and the D -decomposition theory [43], the collapse of the σ -stable region must occur at a triple real root, leading to the following system of equations:

$$\Delta|_{(-\sigma;h)} = 0, \quad (30a)$$

$$\frac{d\Delta}{ds} \Big|_{(-\sigma;h)} = 0, \quad (30b)$$

$$\frac{d^2\Delta}{ds^2} \Big|_{(-\sigma;h)} = 0. \quad (30c)$$

The proof ends by solving the given system (30a)-(30c) for σ under the restriction $\sigma \in \mathbb{R}_+$. QED.

Corollary 1.1: Consider the system described by the transfer function $H_{yu}(s; h)$ in (2) in closed-loop with the PI controller in (5), and assume that the corresponding curve \mathcal{K} does not have self-intersections, then optimal control gains $(\hat{k}_p, \hat{k}_i) \in \mathbb{R}^2$ that place the spectral abscissa $\rho(\Delta)$ as far left as possible are given by:

$$\hat{k}_p = \frac{(-h\hat{\sigma}^4 + c_1\hat{\sigma}^3 - c_2\hat{\sigma}^2 - c_3\hat{\sigma} + bz)}{e^{h\hat{\sigma}}(\hat{\sigma} + z)^2}, \quad (31)$$

where

$$\begin{aligned} c_1 &= ah - hz + 2, & c_2 &= -z(ah + 3) + a + bh, \\ c_3 &= z(2a + bh), \end{aligned}$$

and

$$\hat{k}_i = \frac{\hat{\sigma}^2(\hat{\sigma}(c_4 + c_5z + \hat{\sigma}) - az - b(h(\hat{\sigma} + z) + 1))}{e^{h\hat{\sigma}}(\hat{\sigma} + z)^2}, \quad (32)$$

where

$$c_4 = h\hat{\sigma}(a - \hat{\sigma}), \quad c_5 = ah - h\hat{\sigma} + 2.$$

Proof. The proof is straightforward by solving the system of equations (30a)-(30c) for k_p and k_i . QED.

Theorem 1 allows us to explicitly find the minimal achievable spectral abscissa, while Corollary 1.1 allows us to compute the control gains that guarantee the spectral abscissa to be as far left as possible. However, it also requires the curve to be free of self-intersections. Such a restriction is a major one since we do not have an analytical result that helps us determine when the curve will present such auto-intersection. Nonetheless, we can still find optimal control gains when the curve has this geometrical behavior. More precisely, there are three possible scenarios:

- Case I.** The collapse of the stability region occurs at a triple real root, and the control gains can be computed employing Theorem 1.
- Case II.** The collapse of the stability region occurs at a double complex conjugate root.
- Case III.** The collapse of the stability region occurs at a complex conjugate root + a simple real root.

Figure 8 depicts the behavior of the σ -stable region as the value of σ changes until achieving its maximum value.

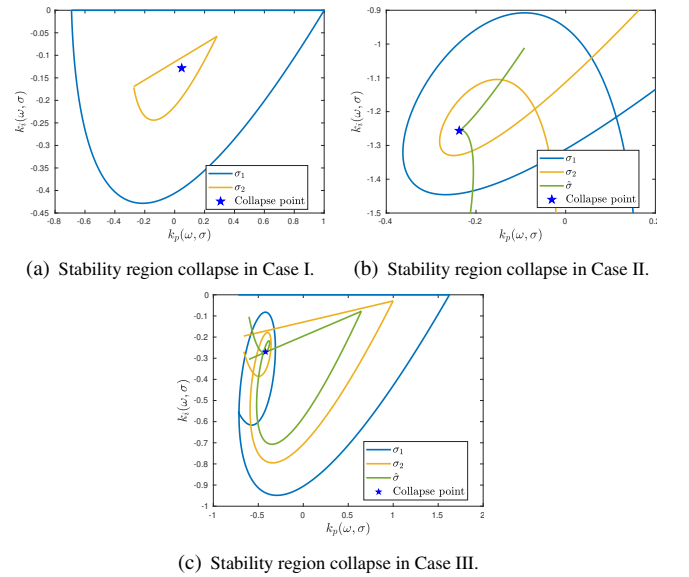
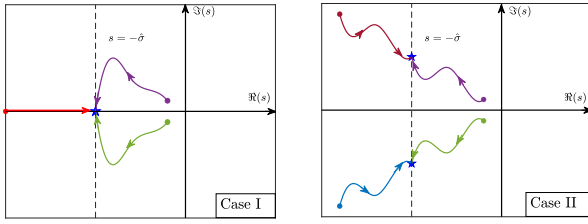


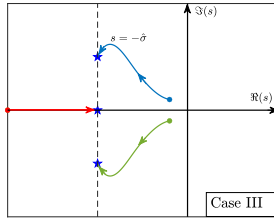
FIGURE 8. Different types of stability region collapse.

It is also interesting to observe how the roots behave in the complex plane as the control parameters change inside the stability region until the collapse point, as depicted in Figures 9(a)-9(c).

Based on the different cases, the following algorithm allows us to find the maximum value of σ such that the stability region \mathcal{S} exists. In order to perform such a task, the algorithm starts by considering an interval of σ values and an interval of crossing frequencies. The results rely on the fact that, for the maximum value of σ , if the crossing curve presents self-intersections, the region \mathcal{S} must be composed of either one



(a) Root behavior and minimum spectral abscissa for Case I. (b) Root behavior and minimum spectral abscissa for Case II.



(c) Root behavior and minimum spectral abscissa for Case III.

FIGURE 9. Roots behavior as the stability region collapses.

crossing frequency $\omega \neq 0$ or by two, one of them being $\omega = 0$. The algorithm is the following:

First, we take an increasing sequence (σ_j) , and define a σ -stability crossing curve $\mathcal{K}_{\sigma_j, \omega}$ corresponding to each of the given σ and $\omega \in \Omega_{\omega_j}$ the set of crossing frequencies for the given σ_j . Next, we verify the existence of a σ -stable region \mathcal{S}_{σ_j} . If it exists, then we compute both the cardinality of the region \mathcal{S}_{σ_j} and the cardinality of the set of intersections between the curve for $\omega \neq 0$ and the line that corresponds to $\omega = 0$. Then, if the cardinality of the region is $\text{card}\{\mathcal{S}_{\sigma_j}\} = 1$, that means the region has already collapsed to a point. Then, we verify what of the different cases the collapse corresponds to by checking the number of intersections. In other words, we are in Case II if there are no intersections since it implies a double complex root. If, on the contrary, there is one intersection, that means that the line corresponding to $\omega = 0$, which at the same time corresponds to a real root, is also part of the collapse, and therefore, we are in Case III. Finally, the σ_j for which the region collapses is the corresponding $\hat{\sigma}$. If we do not find any collapse after computing the region for each σ_j inside the sequence, we reinitialize the procedure considering a larger sequence. The formalization of the Algorithm can be found in Appendix A.

V. PI CONTROLLER FRAGILITY

Just as common as input/output delays and NMP behavior, control systems always have to deal with control fragility, which measures "how robust a controller is with respect to control parameters uncertainties". Such a problem plays an essential role when we consider the implementation of the controller in a real plant. The problem can be stated as

follows:

Problem 2: For a second-order NMP LTI SISO system with transfer function given by (2) in closed-loop with a PI controller given by (5), with given stabilizing control gains $(k_p^*, k_i^*) \in \mathbb{R}^2$, find the maximum controller parameter deviation d , such that the closed-loop system preserves stability as long as the following inequality holds:

$$\sqrt{(k_p - k_p^*)^2 + (k_i - k_i^*)^2} < d. \quad (33)$$

Consider the following function $\gamma : \mathbb{R}_+ \rightarrow \mathbb{R}_+$:

$$\gamma(\omega) := \begin{cases} \sqrt{(k_p(\omega) - k_p^*)^2 + (k_i(\omega) - k_i^*)^2} & \text{if } \omega \in \mathbb{R}_+^* \\ |k_i^*| & \text{if } \omega = 0, \end{cases} \quad (34)$$

Proposition 6: Let \vec{k}^* be a stabilizing controller. Then the maximum controller parameter deviation d , such that the closed-loop system preserves stability, is given by:

$$d = \min_{\omega \in \Omega_c \cup \{0\}} \{\gamma(\omega)\}, \quad (35)$$

where $\Omega_c \subseteq \mathbb{R}_+$ is the set of roots of the function $f : \Omega \rightarrow \mathbb{R}_+$ given by:

$$f(\omega) = \left\langle \vec{k}(\omega) - \vec{k}^*, \frac{d\vec{k}}{d\omega} \right\rangle. \quad (36)$$

Proof. By assumption \vec{k}^* is a stabilizing controller, that is, $\vec{k}^* \in \mathcal{S}$. Therefore, the only possibility to lose stability is by crossing \mathcal{K} , which could be either through \mathcal{K}_ω or \mathcal{K}_0 . First, it is clear that the euclidean distance to \mathcal{K}_0 from any \vec{k}^* with $k_i^* \neq 0$ is given by $\gamma(0)$. Next, the minimal distance from \vec{k}^* to \mathcal{K}_ω is given by the distance to the points where the vector $\vec{k}(\omega) - \vec{k}^*$ is perpendicular to the tangent to the crossing curve \mathcal{K}_ω , that is, whenever $f(\omega) = 0$. It is important to recall that the tangent to the crossing curve is well-defined for any $\omega \neq 0$. Finally, it is clear that for any $\omega \neq 0$, the distance from \vec{k}^* to the crossing curve is given by $\gamma(\omega)$. This last observation ends the proof. QED.

Example 1 (Illustrative example): From [35], we consider the system with transfer function representation given by:

$$\frac{s-1}{s^2+s+1}e^{-s}, \quad (37)$$

for which the optimal gains are depicted in Figure 10. In this figure, it is easy to observe the fragility of the given controller. It is also clear that the *optimal* gains, in terms of the spectral abscissa, do not necessarily correspond to those with *less* fragility. Moreover, it is not clear if the *less* fragile controller ever matches the *optimal* one.

VI. DELAY MARGIN OF STABILIZED CLOSED-LOOP SYSTEMS

Similar to the fragility of the controller, the delay margin of the closed-loop system is a measure of "how large of a delay can the closed-loop system tolerate". Until this point, the delay parameter $h \in \mathbb{R}_+$ has been considered known

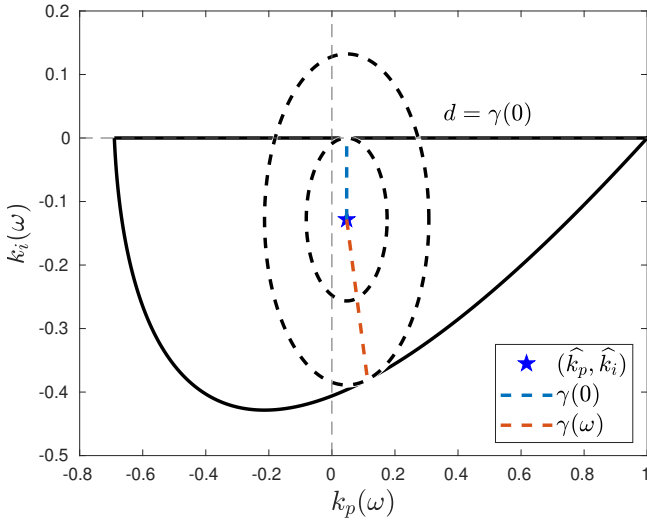


FIGURE 10. Fragility of the optimal controller.

and constant. However, as has already been mentioned, the stability region of the closed-loop system depends on the delay. Therefore, it is interesting to know how much the delay parameter can vary before losing stability for a given stabilizing controller $\vec{k}^* \in \mathcal{S}$. With this in mind, we have the following definition:

Definition 7 (Delay margin): Consider the closed-loop characteristic function $\Delta(s; k_p, k_i, h)$ and its spectral-abscissa $\rho(\Delta)$. Assume that the controller $K(s)$ with gains $\vec{k}^* = (k_p^*, k_i^*)$ is a stabilizing controller. Then the *delay margin* of the closed-loop system is defined by

$$h_{max} := \sup\{\beta \in \mathbb{R}_+ : \rho(\Delta) < 0 \quad \forall h \in [h^*, \beta)\},$$

where h^* is the corresponding delay parameter of the system. Consider the function $F : \mathbb{R}^3 \times \mathbb{R}_+ \rightarrow \mathbb{R}$ given by:

$$F(\omega, k_p, k_i, h) := a^2\omega^4 + (\omega^3 - b\omega)^2 - (\omega^2 + z^2)(k_i^2 + k_p^2\omega^2). \quad (38)$$

We also introduce the set $\Xi \subset \mathbb{R} \times \mathbb{R}_+$ as the set of all pairs (ω^*, h^*) such that, for a given pair (k_p^*, k_i^*) the following system of equations hold:

$$F(\omega^*, k_p^*, k_i^*, h^*) = 0, \quad (39)$$

$$h^*\omega^* = \arg \left\{ \frac{\omega^*(\omega^*(\omega^* - ia) - b)}{(z - i\omega^*)(k_p^*\omega^* - ik_i^*)} \right\}. \quad (40)$$

We have the following result:

Proposition 7: Consider the system described by the transfer function $H_{yu}(s; h)$ in (2) in closed-loop with the PI controller $K(s)$ in (5), and let \vec{k}^2 be a stabilizing pair. Then, the delay margin h_{max} of the closed-loop system is given by:

$$h_{max} := \min_{(\omega, h) \in \Xi} h. \quad (41)$$

Moreover, for $h = h_{max}$ a characteristic root crosses from \mathbb{C}_- to \mathbb{C}_+ at $\omega = \omega^*$, where ω^* correspond to the given pair $(\omega^*, h_{max}) \in \Xi$.

Proof First, it is clear that if $\Delta(i\omega; k_p, k_i, h) = 0$, the following must hold:

$$(i\omega)^3 + a(i\omega)^2 + bi\omega = e^{-hi\omega}((i\omega - z)(k_i + k_p(i\omega)),$$

which leads directly to (39) and (40). Next, since the closed-loop system is assumed to be stable and by the continuity property of the characteristic roots w.r.t. the delay parameter h , the only possible way to lose stability is by crossing the imaginary axis. Moreover, by the same arguments, the smallest h for which there exists such a crossing must be from \mathbb{C}_- to \mathbb{C}_+ . This last observation ends the proof. QED.

VII. NUMERICAL EXAMPLES

Example 2 (Unstable NMP time-delay plant): Consider the open-loop system described by the following transfer function:

$$H_{yu}(s; h) = \frac{s - 1}{(s + 1)(s - 1/10)} e^{-s}. \quad (42)$$

Computing the stability region allows us to observe that we are in Case I, as depicted in Figure 11(b), which means that we can compute the optimal gain by means of Theorem 1. Indeed, considering the control gains $(\hat{k}_p, \hat{k}_i) = (-0.18, -0.0035)$ the spectral abscissa of the system is located at a triple real root at $s = -0.1344$, while the gains $(-0.4, -0.02)$ place it at $s = -0.015 \pm 0.4i$.

For the sake of comprehensiveness, we consider another arbitrary pair of control gains to compare the performance and robustness with. Table 1 summarizes each selected controller's different aspects.

TABLE 1. Different controllers performance for system (42)

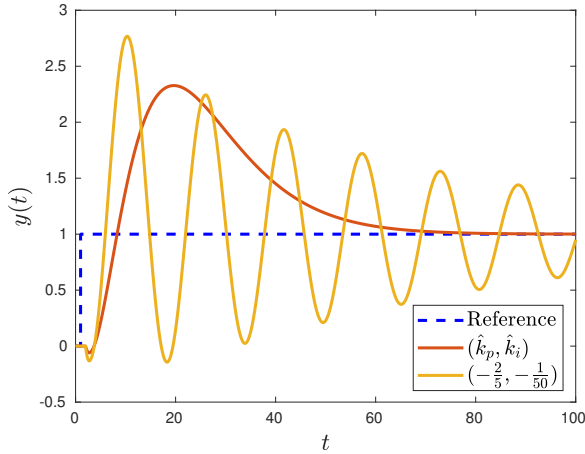
\vec{k}	$\rho(\Delta)$	$d = \min(\gamma(\omega))$	h_{max}
$(\hat{k}_p, \hat{k}_i) = (-0.18, -0.0035)$	-0.1344	0.0035	3.69
$(k_p, k_i) = (-0.4, -0.02)$	-0.015	0.015	1.15

It is worth mentioning that, despite being the *optimal* control gains in terms of the spectral abscissa, selecting $\vec{k} = (-0.18, -0.0035)$ makes the system more fragile. However, when we consider instead the delay margin, which can be easily computed using Proposition 7, we can easily observe that considering (\hat{k}_p, \hat{k}_i) makes the system more resilient to delay variations. Therefore, the selection of the corresponding controller will, in general, depend on the application requirements.

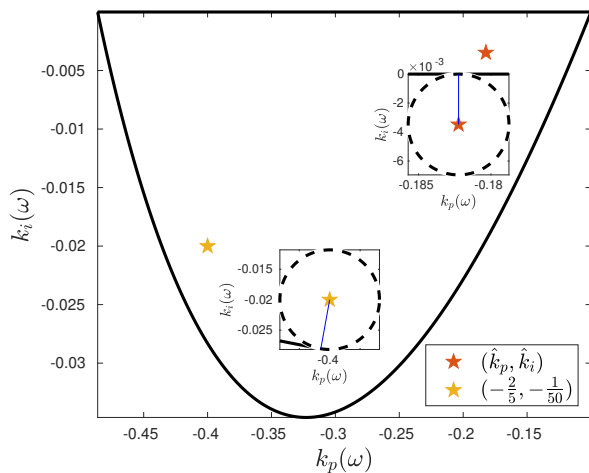
Example 3 (NMP oscillator): Consider the open-loop system with associated transfer function given by:

$$H_{yu}(s; h) = \frac{s - z}{s^2 + \omega_n^2} e^{-hs}, \quad (43)$$

where ω_n is the oscillator frequency. Let us consider $z = 1/2$ and $\omega_n = \sqrt{2}$ with a delay $h = 2/3$. Figure 12(b) depicts the presence of a self-intersection on the corresponding crossing curve \mathcal{K} . Therefore, the collapse corresponds either to Case II or III. Algorithm 1 allows us to identify the collapse as Case II and find the minimum of the spectral abscissa, which



(a) Time response of the closed-loop system.



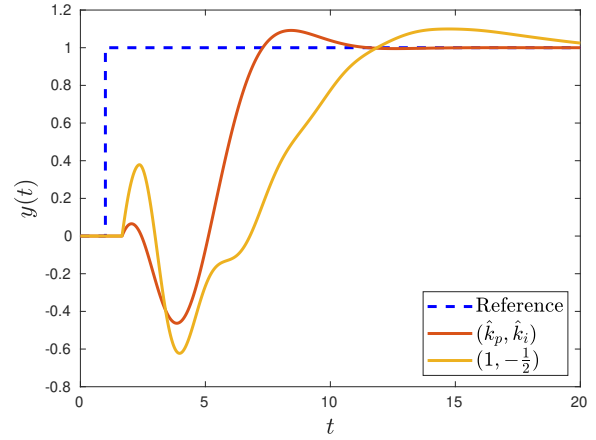
(b) Stability region and selected gains with its corresponding distance to instability d .

FIGURE 11. System (42) in closed-loop with the optimal PI controller vs an arbitrary stabilizing controller.

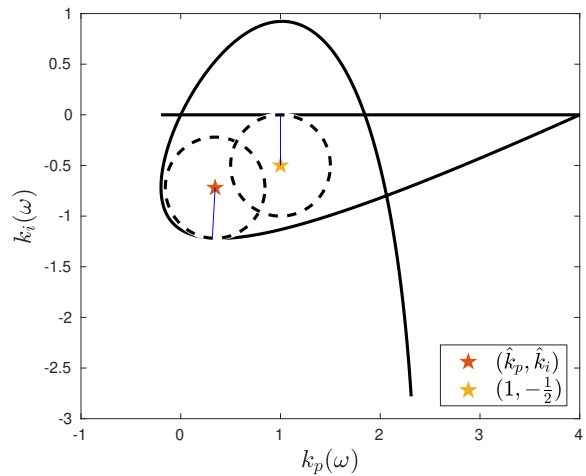
in this case corresponds to $\rho(\Delta) = -0.8$ achieved with the control gains $(\hat{k}_p, \hat{k}_i) = (0.34, -0.71)$. The closed-loop system response for the optimal gains and an additional pair of control gains is shown in Figure 12(a). We can also appreciate the *fragility* of both considered controllers in Figure 12(b). Table 2 summarizes the different aspects of the optimal PI controller and the arbitrary controller $(k_p, k_i) = (1, -1/2)$. One interesting observation is that although both controllers have similar robustness with respect to uncertainties in the control gains and similar tolerances with respect to changes in the delay parameter, the performance in terms of velocity is large.

TABLE 2. Different controllers performance for system (43)

\vec{k}	$\rho(\Delta)$	$d = \min(\gamma(\omega))$	h_{max}
$(\hat{k}_p, \hat{k}_i) = (0.34, -0.71)$	-0.8	0.49	1.60
$(k_p, k_i) = (1, -0.5)$	-0.24	0.5	1.03



(a) Time response of the closed-loop system.



(b) Stability region and selected gains with its corresponding distance d .

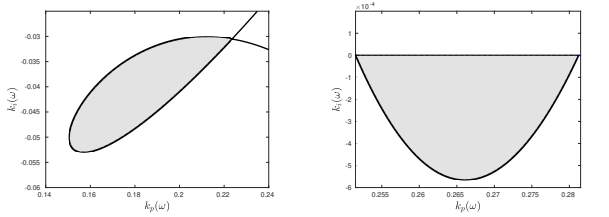
FIGURE 12. System (43) in closed-loop with the optimal PI controller vs an arbitrary stabilizing PI controller.

Example 4 (NMP time-delay system with complex unstable roots): Consider described by the following transfer function:

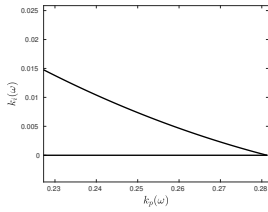
$$H_{yu}(s; h) = \frac{s - 2}{s^2 - \frac{s}{2} + \frac{9}{16}} e^{-2s}. \quad (44)$$

The system open-loop characteristic roots are located at $s = \frac{1}{4} \pm \frac{1}{2}i$. Before finding the corresponding optimal gains, one interesting behavior arises. In Figure 13, we observe changes in the stability region as the input delay decreases. Indeed, first, when the delay decreases from $h = 2$ to $h = 0.5$, we observe a smaller stable region, also implying that any stabilizing controller will be very *fragile*, that is, with very small variations on its value, stability might be lost. Second, when the delay parameter h value decreases to $h = 0.1$, there is no stable region; in other words, a PI controller cannot stabilize the system for the given delay. This means that the delay parameter has a stabilizing effect. In this sense, it would also be natural to consider the input delay as a control parameter [44], producing a delayed PI controller of

the form: $K(s) = e^{-\tau s}(k_p + k_i/s)$, where τ is seen as a control parameter.



(a) Stability region of system (44) in closed-loop with a PI controller. (b) Stability region of system (44) in closed-loop with a PI controller when $h = 0.5$.



(c) Non-existence of any stability region of system (44) in closed-loop with a PI controller when $h = 0.1$.

FIGURE 13. Closed-loop stability crossing curve for different delays.

Algorithm 1 reveals that the maximum achievable decay rate corresponds to $\hat{\sigma} = 0.055$, which is a very slow system. The corresponding gains are $(\hat{k}_p, \hat{k}_i) = (-0.15, -0.05)$, placing the right-most characteristic root at $s = -0.05 \pm \frac{1}{2}i$. *Example 5 (Brief discussion on the maximum multiplicity of a characteristic root):* Consider the following transfer function:

$$H_{yu}(s; h) = \frac{s - z}{s^2 + as + b} e^{-s}, \quad (45)$$

with the following set of parameters:

$$z = \frac{6\sqrt{15}-23}{11}, \quad a = \frac{-10}{7}, \quad b = \frac{19}{7},$$

and consider the PI control $K(s) = k_p + k_i/s$ with the following control parameters:

$$k_p = \frac{-11}{7e}, \quad k_i = \frac{-(6\sqrt{15} + 23)}{7e},$$

where $e = \exp(1)$. Then, the spectral abscissa of the closed-loop system corresponds to a real root of multiplicity five at $s = -1$, which is the largest *over-order* multiplicity smaller than the degree of the quasi-polynomial. Indeed, it is known from [45] that by achieving the maximum multiplicity of the root, we also guarantee that such a root is the right-most root. Note also that, as was mentioned in Section II, the maximum multiplicity of any root is $\deg(\Delta) = 6$. However, in this case, the characteristic quasi-polynomial is of the following form:

$$\Delta(s; k_p, k_i, h) = P_0(s) + e^{-hs}P_1(s),$$

where:

$$P_0(s) = s^3 + as^2 + bs.$$

Thus, the lack of a free term makes it impossible to achieve the multiplicity six.

VIII. PRACTICAL EXAMPLES

Example 6 (Boiler Steam Drum): This process consists of adjusting the boiler feed water to regulate the level in the boiler steam drum. The process transfer function, as by [46], is the following:

$$H_{yu}(s; h) := \frac{-0.2155(s - 2.39)}{s^2 + 0.93s - 0.009} e^{-0.1s}. \quad (46)$$

In [5] and [46], the exponential term is substituted by the Padé approximation, and a PID controller is proposed. Note that the system presents an unstable real root in open-loop. It is worth mentioning that, due to the structure of the transfer function, we will have $k_i > 0$, due to the negative open-loop gain $k = -0.2155$, which can be *absorbed* by the controller. In this case, the optimal gains $(\hat{k}_p, \hat{k}_i) = (0.4583, 0.0374)$ place the spectral abscissa of the closed-loop system at a triple root located at $s = 0.2673$. Table 3 indicates the gains proposed in [5] and [46] for the PID controllers considered.

TABLE 3. Considered controllers

Controller	k_p	k_i	k_d
Optimal PI	0.4583	0.0374	-
Patil <i>et al.</i>	2.341	0.523	2.1616
Shamsuzzoha <i>et al.</i>	3.2306	0.9215	2.5783

In Figure 14, it can be observed that, on the one hand, the proposed controller reduces the undershoot compared to the PID controllers. However, its response is slower due to the absence of the derivative action³. Another feature worth mentioning is the difference in control effort, as well as the use of small gains in the proposed PI controller. Indeed, Figure 15 depicts the control output of the three controllers, and it is easy to observe that including a derivative action dramatically increases the control effort, a situation that often wants to be avoided.

Example 7 (The DC-DC Boost Converter): As a final example, consider the standard DC-DC Boost Converter consisting of a voltage source E , a switching component M , an inductor L , a capacitor C , and a load resistor R as depicted in Figure 16. PI controllers represent an ideal solution to the control problem of this kind of circuit for two main reasons (for further details on the control of DC-DC boost converters via PI controllers, we refer to [47]–[50]). On the one hand, electrical systems often have to work in the presence of high-frequency noise; consequently, the use of derivative controllers is often avoided. On the other hand, one common requirement of the control design for this kind of application is the elimination of steady-state error, which justifies using an integral action. For these reasons, even though the system is open-loop stable, the

³The derivative action was implemented using a filter; therefore, it increases the number of control parameters by two.

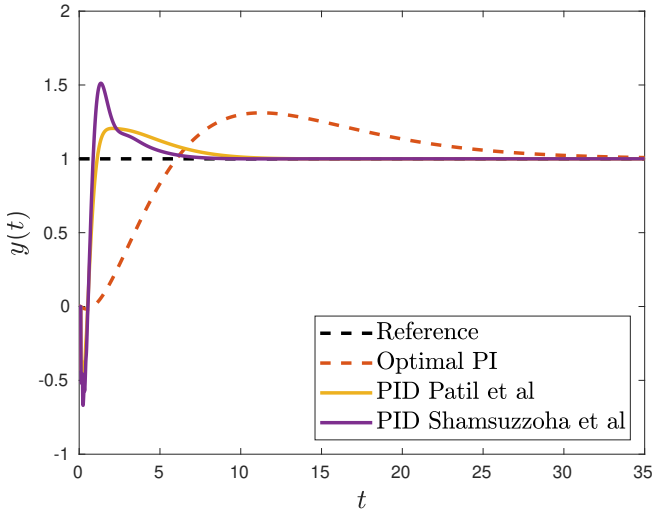


FIGURE 14. Output of system (46) in closed-loop with the proposed PI controller and the PID controllers proposed by Patil et al [5] and Shamsuzzoha et al [46].

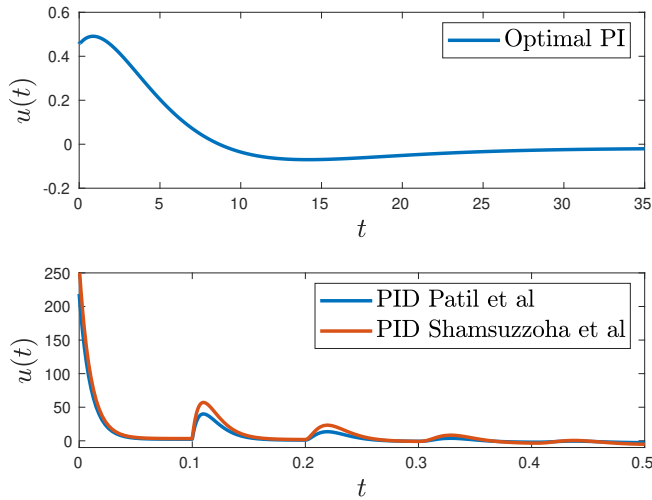


FIGURE 15. Control output the proposed PI controller (up) and the PID controllers proposed by Patil et al. [5], and Shamsuzzoha et al. [46] (down).

design of a closed-loop control strategy remains necessary. One can easily show that the following transfer function describes the output voltage due to the duty cycle:

$$H_{yu}(s) = -\frac{K\omega_0^2(zs-1)}{s^2 + \frac{\omega_0}{Q}s + \omega_0^2} e^{-hs}. \quad (47)$$

The constant $K > 0$ corresponds to a DC gain, $\omega_0 > 0$ is known as the natural frequency, the unstable zero is located at $1/z > 0$, h is an input delay, and $Q > 0$ is referred to as a quality factor. These parameters are characterized by:

$$K = \frac{E}{\eta^2}, \quad \omega_0 = \frac{\eta}{\sqrt{LC}}, \quad z = \frac{L}{\eta^2 R},$$

$$Q = \eta R \sqrt{\frac{C}{L}}, \quad h = 8 \times 10^{-3}$$

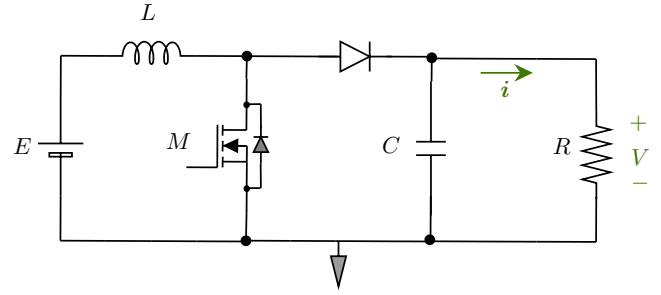


FIGURE 16. DC-DC Boost converter. Circuit described by (47).

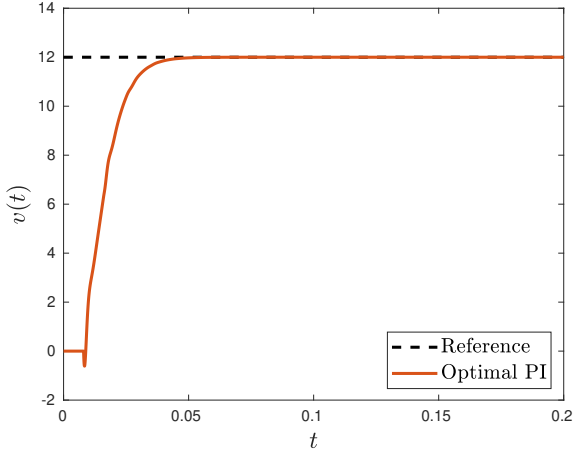
where $\eta := 1 - D$, with D being the duty cycle. In this example we consider $E = 12 \text{ V}$, $D = 0.5$, $C = 10 \mu\text{F}$, $L = 7.05 \text{ mH}$, and $R = 44 \Omega$, which are all standard in the field. By considering Theorem 1, it is easy to observe that the optimal pair corresponds to $(\hat{k}_p, \hat{k}_i) = (0.00278, 1.21478)$. The closed-loop time response of the system is depicted in Figure 17(a). It is worth mentioning that, as observed in Figure 17(b), and in that the optimal value of $k_i = 1.21$, the stable region in this case corresponds to a region where $k_i > 0$. Indeed, this change of sign is due to the negative sign in the transfer function (47).

IX. CONCLUSIONS AND PERSPECTIVES

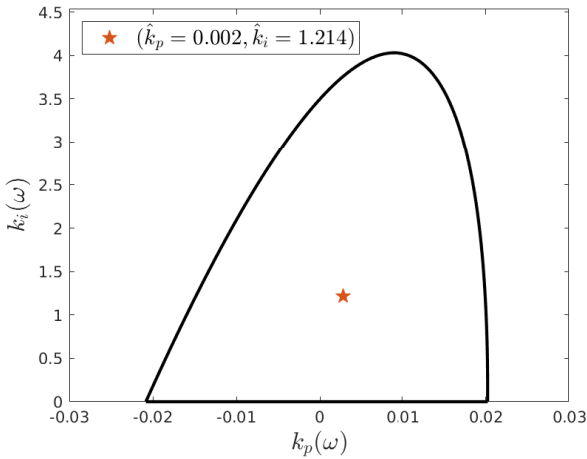
In this note, we presented a systematic procedure that allows optimizing the performance of a second-order non-minimum phase LTI SISO system in terms of its spectral abscissa and, thus, in terms of its decay rate. In this sense, the result was divided into two parts: 1) the case of a triple real root, for which we propose an analytical result that allows finding the exact values of (k_p, k_i) that optimizes the spectral abscissa, under the assumption of a crossing curve with no self-intersections. 2) the case where the stability crossing curve presents self-intersection, leading to two possible scenarios, for which we propose an algorithm that allows finding the optimal gains and distinguishing between the two possible cases. It is worth mentioning that some discussion about the maximum multiplicity of the characteristic roots was also included. Additionally, results regarding the robustness of the controller, both in terms of control parameters and delay uncertainties, were also presented.

The applicability of the presented results to real-world problems was also shown through a pair of practical examples, which included a boiler steam drum and a DC-DC boost converter.

In particular, one interesting perspective is finding the relationship between the multiplicity of a root and its *dominant* behavior, as discussed in Example 5. Future work may also consider a parametric analysis that allows us to determine a priori whether or not a stability region exists and the possible existence and location of self-intersections in the stability crossing curve.



(a) Time response of system (47) in closed-loop with the optimal PI controller.



(b) Stable region of the closed-loop system with the location of the optimal controller.

FIGURE 17. (a) Time-domain response of the optimal PI controller. (b) Location of the optimal PI controller in the stability region.

APPENDIX A ALGORITHM IMPLEMENTATION

ACKNOWLEDGMENT

Diego Torres-García is enrolled in a joint supervision program between the Autonomous University of San Luis Potosi and Paris-Saclay University.

We thank the Associate Editor and the Reviewers for their comments and remarks, which helped us to improve the overall quality of the paper.

REFERENCES

- [1] M. A. Haidekker, *Linear feedback controls: the essentials*. Elsevier, 2020.
- [2] K. Uren and G. van Schoor, "Predictive pid control of non-minimum phase systems;" 2011.
- [3] S. Uma and A. S. Rao, "Enhanced modified smith predictor for second-order non-minimum phase unstable processes," *International Journal of Systems Science*, vol. 47, no. 4, pp. 966–981, 2016.
- [4] P. Patil and C. S. Rao, "Enhanced pid controller for non-minimum phase second order plus time delay system," *Chemical product and process modeling*, vol. 14, no. 3, p. 20180059, 2019.
- [5] P. Patil, S. S. Anchan, and C. S. Rao, "Improved pid controller design for

Algorithm 1: Optimization of the spectral abscissa.

Data: Let \mathcal{S} be a stable region of (6). Let (σ_j) be an increasing sequence in Γ such that $\sigma_0 := \sigma^{(-)}$ and $\sigma_\ell := \sigma^{(+)}$. Let $\mathcal{K}_{\sigma_j, \omega}$ be such that

$$\omega \in \Omega_{\sigma_j} := [\underline{\omega}_{\sigma_j}, \bar{\omega}_{\sigma_j}].$$

Result: The optimal $\hat{\sigma}$.

```

1  $j \leftarrow 0; \Gamma \leftarrow (\sigma_0, \sigma_\ell); flag \leftarrow 1;$ 
2 while  $flag \equiv 1$  do
3    $N_j^{(s)} \leftarrow \text{card} \{ \mathcal{S}_{\sigma_j} \};$ 
4    $N_j^{(k)} \leftarrow \text{card} \{ \mathcal{K}_{\omega, \sigma_j} \cap \mathcal{K}_{0, \sigma_j} \};$ 
5   if  $N_j^{(s)} \equiv 1 \wedge N_j^{(k)} \equiv 0$  then
6      $\hat{\sigma} \leftarrow \sigma_j;$ 
7     Case  $\leftarrow$  Case II;
8      $flag \leftarrow 0;$ 
9   else
10    if  $N_j^{(s)} \equiv 1 \wedge N_j^{(k)} \equiv 1$  then
11       $\hat{\sigma} \leftarrow \sigma_j;$ 
12      Case  $\leftarrow$  Case III;
13       $flag \leftarrow 0;$ 
14     $j \leftarrow j + 1;$ 
15    if  $j > \ell$  then
16      Select new  $\Gamma$  and start again;

```

an unstable second order plus time delay non-minimum phase systems," *Results in Control and Optimization*, vol. 7, p. 100117, 2022.

- [6] R. P. Sree and M. Chidambaram, *Control of unstable systems*. Alpha Science International Ltd., 2006.
- [7] S. Zhao and Z. Gao, "Active disturbance rejection control for non-minimum phase systems," in *Proceedings of the 29th Chinese control conference*. IEEE, 2010, pp. 6066–6070.
- [8] Z. Chen, W. Gao, J. Hu, and X. Ye, "Closed-loop analysis and cascade control of a nonminimum phase boost converter," *IEEE Transactions on power electronics*, vol. 26, no. 4, pp. 1237–1252, 2010.
- [9] K. G. Begum, A. S. Rao, and T. Radhakrishnan, "Enhanced imc based pid controller design for non-minimum phase (nmp) integrating processes with time delays," *ISA transactions*, vol. 68, pp. 223–234, 2017.
- [10] S. K. Pandey, S. L. Patil, and S. Phadke, "Regulation of nonminimum phase dc–dc converters using integral sliding mode control combined with a disturbance observer," *IEEE Transactions on Circuits and Systems II: Express Briefs*, vol. 65, no. 11, pp. 1649–1653, 2017.
- [11] R. E. Bellman and K. L. Cooke, "Differential-difference equations," 1963.
- [12] K. Gu, V. Kharitonov, and J. Chen, *Stability of time-delay systems*. Boston: Birkhauser, 2003.
- [13] W. Michiels, K. Engelborghs, D. Roose, and D. Dochain, "Sensitivity to infinitesimal delays in neutral equations," *SIAM Journal on Control and Optimization*, vol. 40, no. 4, pp. 1134–1158, 2002.
- [14] R. Sipahi, S.-I. Niculescu, C. Abdallah, W. Michiels, and K. Gu, "Stability and stabilization of systems with time delay," *IEEE Control Systems Magazine*, vol. 31, no. 1, pp. 38–65, 2011.
- [15] L. Pekař and Q. Gao, "Spectrum analysis of lti continuous-time systems with constant delays: A literature overview of some recent results," *IEEE Access*, vol. 6, pp. 35 457–35 491, 2018.
- [16] G. J. Silva, A. Datta, and S. P. Bhattacharyya, *PID controllers for time-delay systems*. Springer Science & Business Media, 2007.
- [17] M. Shamsuzzoha, J. Jeon, and M. Lee, "Improved analytical pid controller design for the second order unstable process with time delay," in *Computer Aided Chemical Engineering*. Elsevier, 2007, vol. 24, pp. 901–906.
- [18] N. Hohenbichler, "All stabilizing pid controllers for time delay systems," *Automatica*, vol. 45, no. 11, pp. 2678–2684, 2009.
- [19] V. A. Oliveira, L. V. Cossi, M. C. Teixeira, and A. M. Silva, "Synthesis

- of pid controllers for a class of time delay systems,” *Automatica*, vol. 45, no. 7, pp. 1778–1782, 2009.
- [20] L. R. da Silva, R. C. C. Flesch, and J. E. Normey-Rico, “Controlling industrial dead-time systems: When to use a pid or an advanced controller,” *ISA transactions*, vol. 99, pp. 339–350, 2020.
- [21] C.-F. Méndez-Barrios, S.-I. Niculescu, and A. Martínez-González, “Characterizing some improperly posed problems in proportional-derivative control,” *International Journal of Robust and Nonlinear Control*, vol. 32, no. 18, pp. 9452–9474, 2022.
- [22] C.-F. Méndez-Barrios, J.-D. Torres-García, and S.-I. Niculescu, “Delay-difference approximations of pd-controllers. improperly-posed systems in multiple delays case,” *International Journal of Robust and Nonlinear Control*, vol. 34, no. 10, pp. 6431–6454, 2024. [Online]. Available: <https://onlinelibrary.wiley.com/doi/abs/10.1002/rnc.7217>
- [23] W. Michiels, “To filter or not to filter? impact on stability of delay-difference and neutral equations with multiple delays,” *IEEE Transactions on Automatic Control*, 2022.
- [24] G. A. Baker and P. Gaves-Morris, *Essentials of Padé approximants*. Edinburgh, UK: Cambridge University Press, 2007.
- [25] Y. Tian and Z. Wang, “Stability analysis and generalized memory controller design for delayed t-s fuzzy systems via flexible polynomial-based functions,” *IEEE Transactions on Fuzzy Systems*, vol. 30, no. 3, pp. 728–740, 2020.
- [26] F. Mazenc, S.-I. Niculescu, and D. Torres-García, “Stability analysis for linear systems with a switched rapidly varying delay,” *Automatica*, vol. 169, p. 111862, 2024.
- [27] W. Zhang, M. S. Branicky, and S. M. Phillips, “Stability of networked control systems,” *IEEE control systems magazine*, vol. 21, no. 1, pp. 84–99, 2001.
- [28] Y. I. Neimark, “Structure of the d-partition of the space of polynomials and the diagram of vishnegradskii and nyquist,” in *Dokl Akad Nauk SSSR*, vol. 59, 1948, p. 853.
- [29] E. Pinney, *Ordinary difference-differential equations*. Univ of California Press, 1958.
- [30] J. Ackermann, “Parameter space design of robust control systems,” *IEEE Transactions on Automatic Control*, vol. 25, no. 6, pp. 1058–1072, 1980.
- [31] M.-T. Ho, A. Datta, L. Keel, and S. Bhattacharyya, “Robust and optimal pid controller design,” *IFAC Proceedings Volumes*, vol. 30, no. 16, pp. 55–60, 1997.
- [32] M. S. Lee and C. Hsu, “On the τ -decomposition method of stability analysis for retarded dynamical systems,” *SIAM Journal on Control*, vol. 7, no. 2, pp. 242–259, 1969.
- [33] W. Michiels and S.-I. Niculescu, *Stability, control, and computation for time-delay systems: an eigenvalue-based approach*. SIAM, 2014.
- [34] A. Ramírez, S. Mondié, R. Garrido, and R. Sipahi, “Design of proportional-integral-retarded (pir) controllers for second-order lti systems,” *IEEE Transactions on Automatic Control*, vol. 61, no. 6, pp. 1688–1693, 2015.
- [35] D. Torres-García, C.-F. Méndez-Barrios, S.-I. Niculescu, and M. Hernández-Gómez, “Pi control for optimal spectral abscissa in general non-minimum phase systems with time delay,” in *2024 10th International Conference on Control, Decision and Information Technologies (CoDIT)*, 2024, pp. 1358–1363.
- [36] F. Wielonsky, “A Rolle’s Theorem for Real Exponential Polynomials in the Complex Domain,” *J. Math. Pures Appl.*, vol. 80, no. 4, pp. 389–408, 2001.
- [37] D. Torres-García, F. Méndez-Barrios, and A. Ramírez, “Maximum exponential decay rate for first-order time-delay systems with pi controllers,” in *Advances in Automation and Robotics Research: Proceedings of the 3rd Latin American Congress on Automation and Robotics, Monterrey, Mexico 2021*. Springer, 2022, pp. 34–42.
- [38] D. Ma, I. Boussaada, J. Chen, C. Bonnet, S.-I. Niculescu, and J. Chen, “Pid control design for first-order delay systems via mid pole placement: Performance vs. robustness,” *Automatica*, vol. 137, p. 110102, 2022.
- [39] I. Boussaada, G. Mazanti, and S.-I. Niculescu, “The generic multiplicity-induced-dominancy property from retarded to neutral delay-differential equations: When delay-systems characteristics meet the zeros of kummer functions,” *Comptes Rendus. Mathématique*, vol. 360, no. G4, pp. 349–369, 2022.
- [40] J.-E. Hernández-Díez, C.-F. Méndez-Barrios, and S.-I. Niculescu, “Proportional-delayed controllers design for lti-systems: a geometric approach,” *International Journal of Control*, vol. 91, no. 4, pp. 907–925, 2018.
- [41] S. G. Krantz and H. R. Parks, *The implicit function theorem: history, theory, and applications*. Springer Science & Business Media, 2002.
- [42] H. Cheriha, Y. Gati, and V. P. Kostov, “Degree 5 polynomials and descartes’ rule of signs,” *series Mathematics*, p. 3, 2020.
- [43] E. N. Gryazina, “The d-decomposition theory,” *Automation and Remote Control*, vol. 65, no. 12, pp. 1872–1884, 2004.
- [44] J.-E. Hernández-Díez, C.-F. Méndez-Barrios, S.-I. Niculescu, and E. Bárcenas-Bárcenas, “A current sensorless delay-based control scheme for mppt-boost converters in photovoltaic systems,” *IEEE Access*, vol. 8, pp. 174 449–174 462, 2020.
- [45] I. Boussaada, G. Mazanti, S.-I. Niculescu, and A. Benarab, “Mid property for delay systems: Insights on spectral values with intermediate multiplicity,” in *2022 IEEE 61st Conference on Decision and Control (CDC)*. IEEE, 2022, pp. 6881–6888.
- [46] M. Shamsuzzoha and M. Lee, “Pid controller design for integrating processes with time delay,” *Korean Journal of Chemical Engineering*, vol. 25, pp. 637–645, 2008.
- [47] J. Alvarez-Ramírez, I. Cervantes, G. Espinosa-Perez, P. Maya, and A. Morales, “A stable design of pi control for dc-dc converters with an rhs zero,” *IEEE Transactions on Circuits and Systems I: Fundamental Theory and Applications*, vol. 48, no. 1, pp. 103–106, 2001.
- [48] A. Mamizadeh, N. Genc, and R. Rajabioun, “Optimal tuning of pi controller for boost dc-dc converters based on cuckoo optimization algorithm,” in *2018 7th international conference on renewable energy research and applications (ICRERA)*. IEEE, 2018, pp. 677–680.
- [49] P. Warriar, P. Shah, and R. Sekhar, “A comparative performance evaluation of a complex-order pi controller for dc-dc converters,” *Results in Control and Optimization*, vol. 15, p. 100414, 2024.
- [50] J.-A. Hernández-Gallardo, C.-F. Méndez-Barrios, J.-E. Escalante-Martínez, and E. J. Gonzalez-Galvan, “Stabilizing second-order non-minimum phase systems via p̄di controller,” in *2024 10th International Conference on Control, Decision and Information Technologies (CoDIT)*, 2024, pp. 1849–1854.



DIEGO TORRES-GARCÍA was born in San Luis Potosí, Mexico (1994). He is a PhD candidate in a joint supervision program between the University of Paris-Saclay and the Autonomous University of San Luis Potosí (UASLP). He holds a degree in Electronics Engineering from the Faculty of Science of the Autonomous University of San Luis Potosí and a Master of Science in Electrical Engineering from the Faculty of Engineering of the same institution. His research interests include the

stability of dynamical systems with time-delay and the design of delay-based controllers.



SILVIU-IULIAN NICULESCU (FELLOW, IEEE)

received a B.S. degree from the Polytechnical Institute of Bucharest, Romania, the M.Sc. and Ph.D. degrees from the Institut National Polytechnique de Grenoble, France, and the French Habilitation (HDR) from Université de Technologie de Compiègne, all in Automatic Control, in 1992, 1993, 1996, and 2003, respectively. He is currently Research Director at CNRS (French National Center for Scientific Research), L2S (Laboratory of Signals and Systems), a joint research unit of CNRS with CentraleSupélec and Université Paris-Saclay located at Gif-sur-Yvette. Dr. Niculescu is a member of the Inria team “DISCO” and he was the head of L2S for a decade (2010-2019). He is author/coauthor of 11 books and of more than 525 scientific papers. His research interests include delay systems, robust control, operator theory, and numerical methods in optimization, and their applications to the design of engineering systems. He was the Chair of the IFAC TC “Linear Control Systems” (2017–2023), and he served as Associate Editor for several journals in Control area, including the IEEE Transactions on Automatic Control (2003-2005). IEEE Fellow since 2018, Doctor Honoris Causa of University of Craiova (Romania, 2016) and University Low Danube of Galați (Romania, 2023), Founding Editor and Editor-in-Chief of the Springer Nature Series “Advances in delays and dynamics” since its creation in 2012, Dr. Niculescu was awarded the CNRS Silver and Bronze Medals for scientific research and the Ph.D. Thesis Award from Grenoble INP (France) in 2011, 2001 and 1996, respectively.

...



CÉSAR-FERNANDO MÉNDEZ-BARRIOS received the M.Sc. degree in control theory from the Center for Research and Advanced Studies, National Polytechnic Institute (CINVESTAV), in 2005, and the Ph.D. degree from the University of Paris-Sud XI, in 2011. Since 2012, he has been a Professor with the Mechatronics Department, Autonomous University of San Luis Potosí (UASLP). He is currently serving as an Associate Chair of the Graduate Program in Electrical Engineering.

He has authored or coauthored over 60 peer-reviewed publications. His research interest belongs to the qualitative theory of dynamical systems and its application in control problems. More precisely, he is interested by the qualitative analysis of the effects induced by the parameters on the systems dynamics with a particular emphasis on delays as well as the applications of these techniques to the control of robotic and teleoperation systems.